NATIONAL AERONAUTICS A
Washington, D. C.

NASA Grant NGL 44-012-006

CALIBRATION PROGRAM FOR THE 16-FOOT ANTENNA

J. R. Cogdell

Technical Report No. NGL-006-69-1
15 January 1969

Submitted by

Electrical Engineering Research Laboratory

MILIMETER WAVE SCIENCES

The University of Texas at Austin

Austin, Texas

NATIONAL AERONAUTICS AND SPACE ADMINISTRATION
Washington, D. C.

NASA Grant NGL 44-012-006

CALIBRATION PROGRAM FOR THE 16-FOOT ANTENNA

J. R. Cogdell

Technical Report No. NGL-006-69-1
15 January 1969

Submitted by

Electrical Engineering Research Laboratory
MILLIMETER WAVE SCIENCES

The University of Texas at Austin
Austin, Texas

ACKNOWLEDGEMENT

The author would like to acknowledge the aid of the following students in performing the work summarized in this report: E. C. Jelks (USN, Newport, R.I.), Larry Payne (Radiation, Inc., Melbourne, Fla.), John H. Davis, Archie M. Croom, and W. T. Eckert, and also the aid of Mr. C. W. Tolbert, who was responsible for the design of most of the equipment used in these tests.

This work is sponsored by the National Aeronautics and Space Administration, Washington, D.C., under Grant NGL 44-012-006.

TABLE OF CONTENTS

LIST OF FIGURES

I. INTRODUCTION

A. Nature of Work and Scope of this Report.

The present report is concerned with the calibration of the major instrument at the Millimeter Wave Observatory, Mt. Locke - a 16 foot diameter parabolic reflector of high precision. This reflector is the primary component in a radio telescope operative in the millimeter wavelength region. Its calibration was undertaken by a team of four personnel from Electrical Engineering Research Laboratory in Austin, Texas during the summer months of 1967 and 1968.

The data produced by a scientific instrument can be trusted only so far as that instrument's performance is understood and calibrated. The initiation of any major scientific facility is therefore marked by a period of time in which the instruments themselves are under study. Such a period of calibration is indespensible to the eventual successful operation of the facility in scientific inquiry.

The final calibration of an instrument like the 16-foot radio telescope should involve a highly detailed knowledge of its properties. For example, not only should one know the absolute gain, pattern, and pointing accuracy of the antenna, but one should have considerable knowledge of the effects of the environment and the antenna position of these properties. Furthermore such information should be known at all the frequencies where the antenna is potentially useful.

The present study is much more limited in its scope. Specifically, this report is concerned with the absolute gain and pattern of the antenna at three frequencies of operation, 35 GHz, 70 GHz and 97 GHz. A small amount of work was done on a study of the stability of the antenna at 35 GHz and this will be reported, too. Also, sections on antenna pointing accuracy and site evaluation are included. First, we feel it proper to describe the antenna, its history, and its present location.

B. The Antenna

The antenna is shown in Figure 1. It is a parabolic reflector of 16 foot diameter. The feed and the receiver front end are located at the prime focus and are supported by four spars. The antenna is supported by a polar mount, with the polar axis aligned with the earth's axis of rotation. As shown, the antenna is protected from weather by an astrodome.

The motion of the antenna about its two axes of rotation is produced and controlled by electrical servo systems. The details of these systems are not particularly germane to the purpose of this report. It is sufficient to say that the antenna could be driven at a uniform rate of rotation about both axes. The antenna and mount systems are described in more detail in Ref. 1.

Three receivers were used in the measurements. All were of the same general type and they differed primarily in the frequency of operation. The same i.f. amplifier, detector, and recording apparatus was used with all

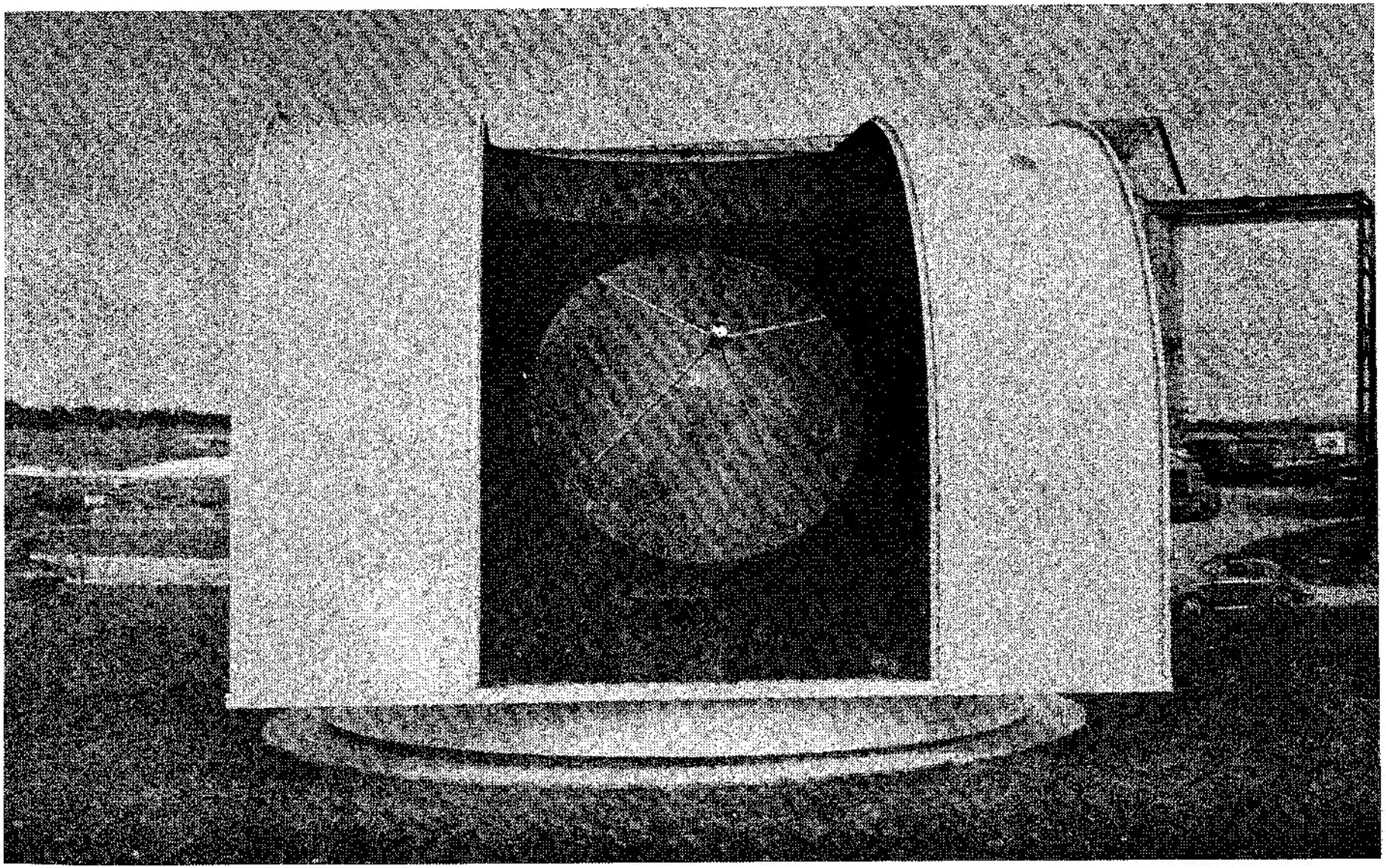

16 FOOT ANTENNA AND ASTRODOME

Fig. 1.

three receiver front ends. The receiver configuration is shown in Fig. 2 and is of superheterodyne type with no r.f. amplification. The second detector is an approximate square law detector, and the i.f. amplifier was operated in a logarithmic mode, such that the output of the receiver was roughly proportional to the logarithm of the input power.

C. The Antenna's Present Location

The antenna was built by the Western Development Laboratory of the Philco-Ford Corporation. It was originally installed at the Balcones Research Center of The University of Texas at Austin, Texas in June 1963. The antenna was used in radio astronomy research at the Austin location until October 1966.[2-5] At that time it was decided to relocate the antenna on Mt. Locke, near Fort Davis, Texas in order to benefit from the superior climate of this locality. The antenna was then taken to Palo Alto, California, for resurfacing while the Mt. Locke site was being developed. The antenna was reinstalled on its mount in April 1967. Testing of the antenna was begun in June 1967. After an intensive testing program during the summer months, the work carried over into the winter months. During the long school session of 1967-68, the author made ten trips to Mt. Locke on weekends and holidays in connection with the antenna calibration program. Then again in the summer months of 1968, a crew in residence resumed an intensive program. This report is concerned with the major results of this work. The calibration program is ongoing, so the results detailed herein must be regarded as somewhat tentative, as will be emphasized in a number of sections.

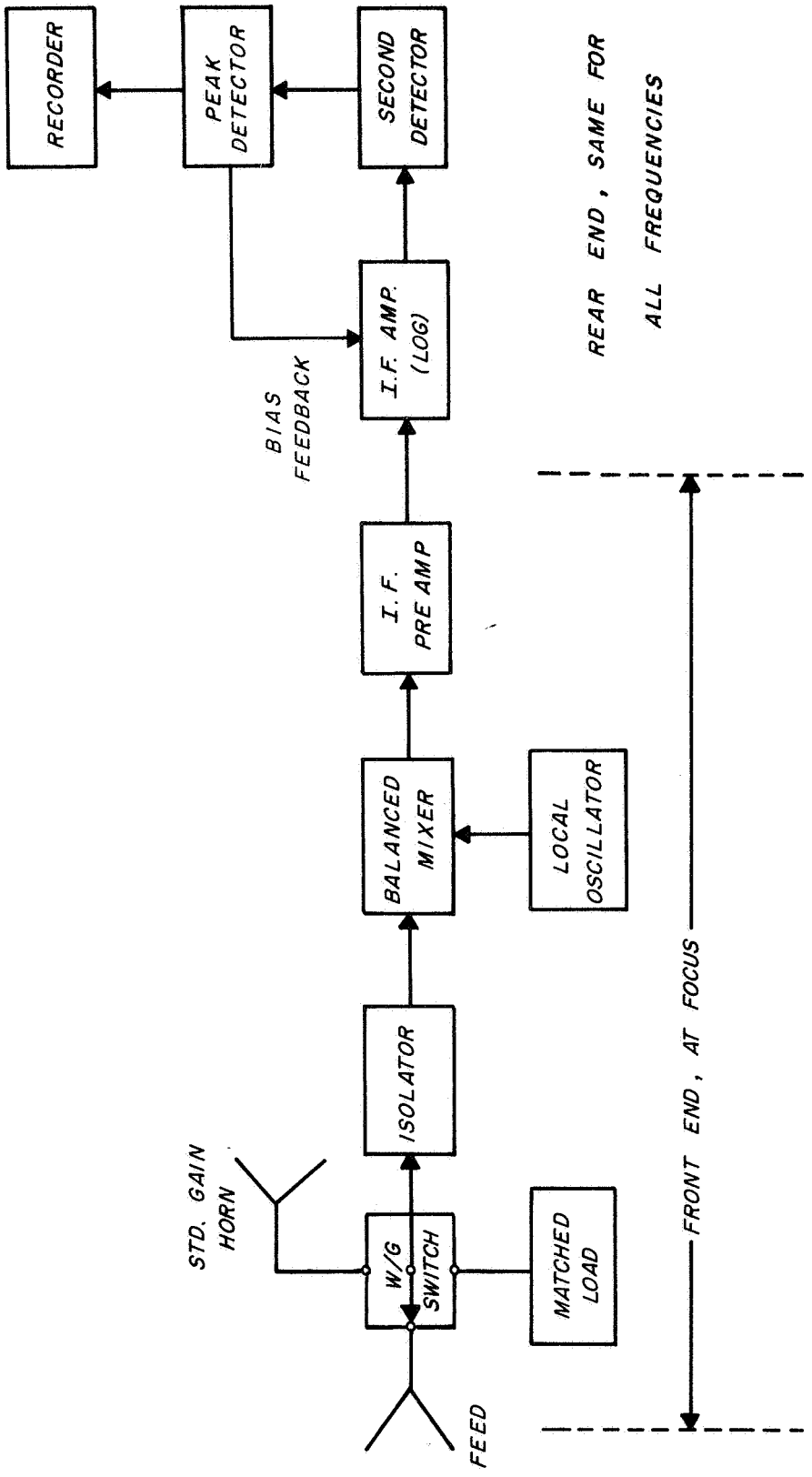

RECEIVER CIRCUIT

Fig. 2.

For the present report, the antenna's location considered as a "pattern range" is of most importance. For purposes of antenna measurements, a transmitter was located in the Davis Mountain State Park, approximately eight miles distance from the antenna site. A profile of the path is shown in Fig. 3, and the transmitter circuit is shown in Fig. 4. Of particular interest in this profile is the general height of the line-of-sight propagation path above the intervening terrain. This property of the range insures that surface meteorological effects on the range properties will be minimal. Also of interest is the ridge located approximately half way between the transmitter and receiver. This ridge acts as a screen to eliminate a reflected wave. The properties of the antenna range are discussed in the following section.

II. EVALUATION OF THE ANTENNA RANGE

A. Uniformity of the Aperture Field

The accuracy of gain measurements of the antenna depended on whether or not transmitted radiation reflected from the surrounding terrain interferred appreciably with the direct radiation at the antenna. This effect was important because the reference gain horns used would be unable to discriminate against incoming reflected waves at small angles, whereas the large antenna would respond only to the direct wave.

Consequently, the transmitter site was chosen to minimize the amount of transmitted signal reflected to the antenna. A profile of the propagation path between the antenna and the transmitter is shown in Fig. 3.

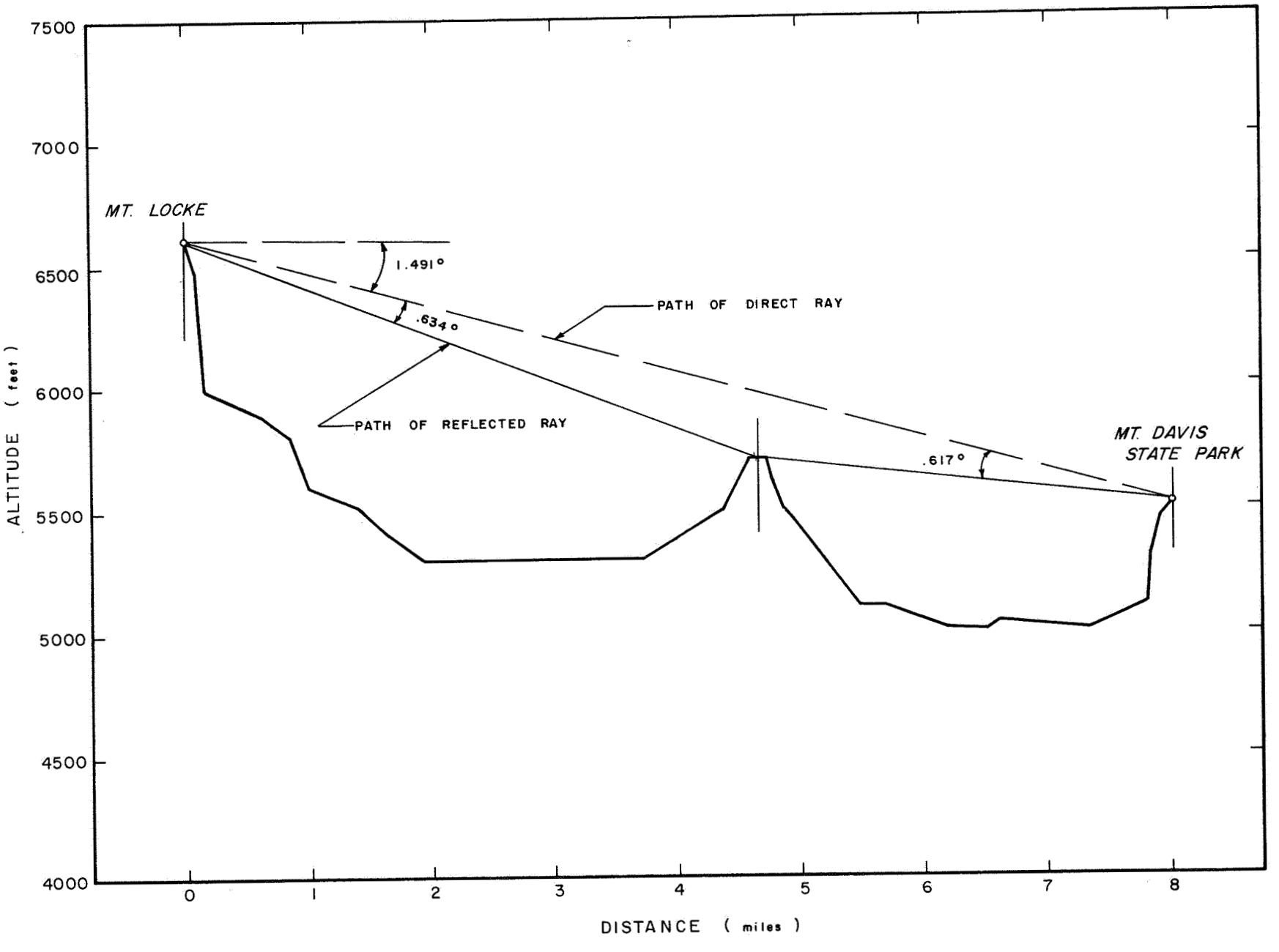

ANTENNA RANGE PROFILE

Fig. 3.

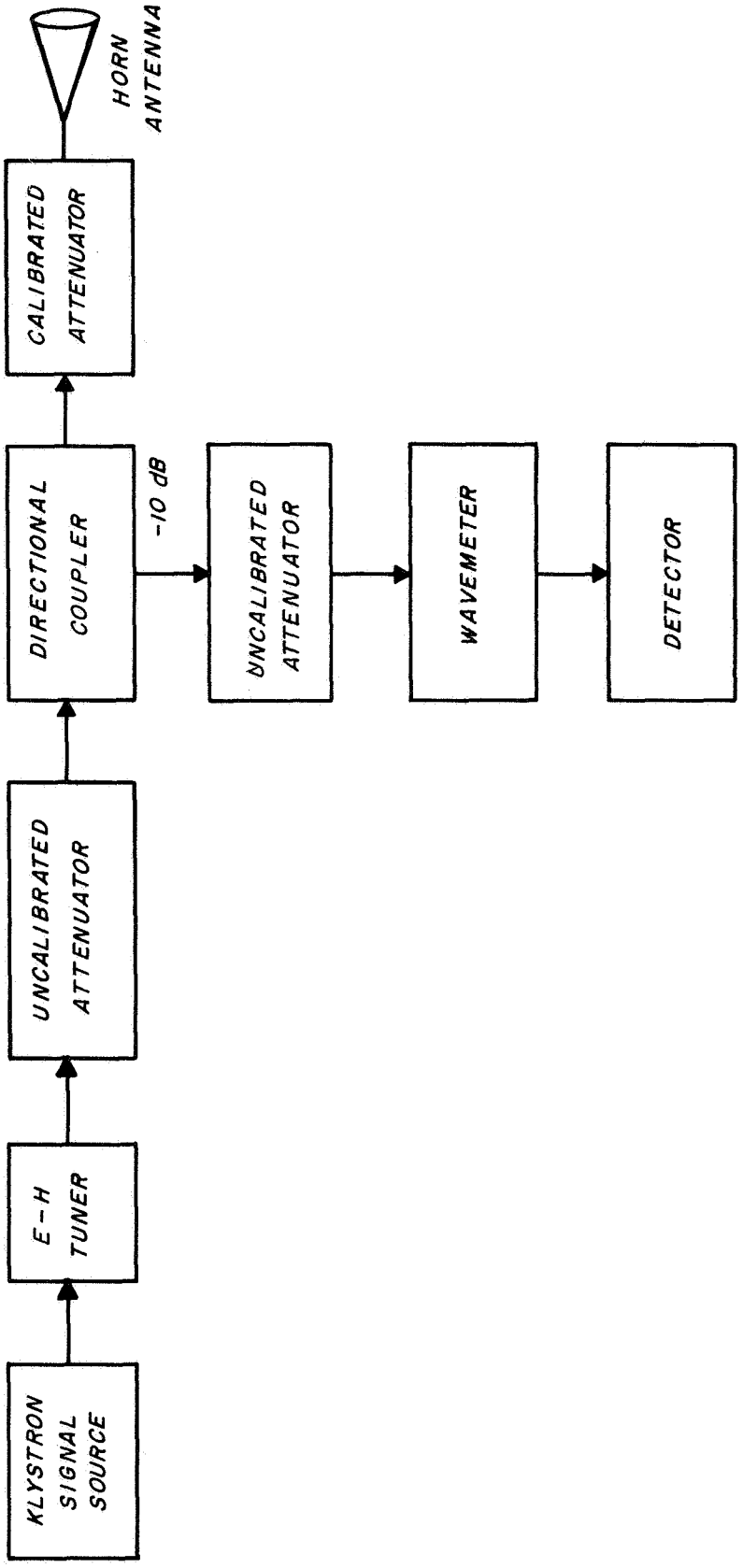

TRANSMITTER CIRCUIT

Fig. 4.

Since the beamwidth of the transmitting antenna is approximately 2° at 8.6 mm, its pattern cannot be depended upon to eliminate the reflected wave. Thus, we undertook a measurement of the reflected wave at 8.6 mm, which represents the worst case of the three wavelengths of interest.

The aperture field of the antenna was probed vertically with the horn at 8.6 mm by continuously recording the signal level while moving the receiver vertically. The geometry leads one to expect an interference pattern in the vertical field due to an interaction of the direct and reflected waves. The geometry suggests a spatial wavelength of $\lambda / \sin 0.634° = 2.4$ feet (see Fig. 3). Accordingly, the vertical field data were Fourier analysed for a period of 2.4 feet, with the results indicating interference magnitudes of 0.05 dB and 0.04 dB for vertical and horizontal polarizations, respectively. These magnitudes indicate that the reflected waves are 46 dB and 48 dB weaker than the direct waves. Thus we see that such effects are negligible compared with other errors in the gain measurements. Furthermore, a statistical analysis indicated that one could expect magnitudes comparable to those indicated by the data from the noise component alone. Thus probabilities are for an even smaller reflected wave than that indicated by the data.

B. Signal Fluctuations

In the previous section we have discussed the effects of the antenna range profile. In the present section we discuss the effects that

the propagation medium (the troposphere) has on the use of the antenna. One effect of the medium is to introduce stochastic fluctuations in the received power level, as indicated by the output of the receiver. These fluctuations are in general non-stationary and highly dependent upon local meteorological conditions.

We have several reasons for discussing these phenomena in this report. For one, there are some highly interesting effects here and they deserve mention for the record's sake. For another, these fluctuation effects placed certain limitations on our work: telling us, for example, when we could make certain kinds of measurements. For yet another, the results obtained could well depend in part on these effects.

1. Source of the Fluctuations

The source of the signal fluctuations is unquestionably meteorological in nature. As the energy of the transmitted wave makes its way from the transmitter to the receiver, it must pass through a nonhomogeneous, time-varying medium. The effect of this medium is to introduce stochastic variations in both the amplitude and phase of the waves at a given point in space. Furthermore, the fluctuations would be expected to be correlated from point to point in a fashion which depends upon the geometry as well as the nature of the medium.

The antenna performs a weighted, coherent addition of the energy falling upon its aperture. Thus the energy entering the receiver shares

this fluctuating quality. Of course, the receiver adds noise and hence adds fluctuations of its own, but these fluctuations were negligible and have a different spectral content compared with the meteorological fluctuations in the measurements. While it is not our purpose to propose a meteorological model for the medium, it is perhaps appropriate to mention that fluctuations seemed to depend upon water vapor content of the atmosphere, wind velocity, local meteorological disturbances (such as clouds), and time of day. These effects are discussed further in the following section.

2. Nature of the Fluctuations

The statistical fluctuations of the signals were on many occasions manifestly non-stationary. It was usually possible to distinguish two components of the fluctuations - one of a non-stationary and slowly varying nature and the other of a stationary nature. These we shall discuss in turn.

The non-stationary component was not always present, but seemed to be related to local meteorological events. For example, the non-stationary component was strongly in evidence when: the shadow of a cloud passed through the propagation path; fog or rain was present in the path; and at sunrise or (to a lesser extent) sunset. It might also be said that this component of fluctuation was present generally in the daytime and when there were large amounts of water vapor in the air.

The stationary component of the fluctuation was always present although the strength of the component was highly variable, depending

upon meteorological conditions. In particular the fluctuations were high when there was much water vapor in the air, the wind was high, and it was daytime. To state extremes, when all three conditions were met signal fluctuations were as high as 3 dB peak-to-peak. When none of the conditions were met, approximately 0.2 dB peak-to-peak fluctuations were experienced. We were forced to adopt a night-time schedule for careful measurements because both components of the noise were lower at night.

It is interesting to note that the fluctuations recorded by the receiver depended upon the size of the antenna furnishing the energy to the receiver. In our work we routinely compared signals received by the 16-foot antenna with signals received by a 3 inch horn antenna, the former signals being suitably reduced such that the received power was roughly the same for the two (see Section V, this report). This procedure naturally led us to compare fluctuations in signals in the two cases. Normally the fluctuations were approximately equal for the two antennas. This indicates that the wave fluctuations are primarily amplitude (as opposed to phase) fluctuations and that such fluctuations are well correlated over the aperture of the 16-foot antenna.

It was not unusual, however, to record larger fluctuations on the 16-foot antenna than on the horn antenna. This indicates that phase decorrelations are dominant and that the critical length of decorrelation is somewhere between the aperture sizes of the two antennas in use.

On a few rare occasions, the fluctuations on the horn seemed to be larger than those on the 16-foot antenna. Such a phenomenon occurred once on a dry, clear, windy day. This would seem to indicate that the fluctuations are primarily amplitude fluctuations and the the fluctuations decorrelate over a length somewhere between the two antenna sizes.

Thus we see that a variety of phenomena can occur. How these effects affect the measurements is an unanswered question, however. Intuitively one would expect that the amplitude fluctuations would average out to the time signal level and that measurements would be unaffected so long as sufficient integration time is permitted. On the other hand, phase decorrelations can only reduce the average signal and one would suspect that the antenna most sensitive to phase decorrelations, viz, the larger antenna, would experience a loss in gain due to such effects. Thus one might anticipate a bias in gain which is dependent on the nature and strength of the fluctuations. Accordingly, all careful gain measurements were made under conditions where fluctuations were minimal. This required predawn hours and relatively low water vapor content.

III. FOCUSING OF THE ANTENNA

A. Principles Used in Focusing

A perfectly parabolic reflector has a unique focus. With the feed properly positioned at that focus, the sidelobes in each principle plane are symmetric, the gain is at its maximum, and, if the feed design is optimum,

the sidelobe levels and beamwidth in the principle planes are approximately equal: in a word, everything is perfect. With a real reflector which is not perfectly parabolic, the "correct" focus may not be easily identified, and one must first decide on a criterion for correctness before the search for the correct focus can begin.

In the present instance three criteria were used in focusing, with results which varied somewhat. One criterion used was concerned solely with the first sidelobes in the principle planes. Specifically, we sought to place the feed at the position which resulted in all four principal sidelobes being at the same level. This criterion has the advantage of being fairly easy to apply when the sidelobes are distinct from the main lobe and of similar structure. Furthermore, this is a criterion which is sensitive to small errors in feed placement and in a sense which indicates the nature of the error.

When an antenna is operated near the limits of its useful range, however, this criterion is not so easily applied on the 16-foot antenna. This is so because in this region the sidelobes are neither distinct from the main lobe nor are they similar in structure. Thus one cannot always identify what is a sidelobe and what its proper level is. In the present case, the chosen criterion was adequate for focusing at 8.6 mm and 4.3 mm wavelength but was of doubtful usefulness at 3.2 mm wavelength.

The two other criteria used were that of equal beamwidths in the principal planes and that of maximum gain. The beamwidth criterion

was subject to too many ambiguities and was difficult to interpret in terms of what to do next. The gain criterion seeks to maximize an important parameter, but proved to be difficult to implement due to the long amount of time required to make a gain measurement. In the two methods described in this paragraph, sidelobes were used as a secondary criterion. Currently we are undecided as to the optimum criterion and procedure for focusing the antenna. We are now studying defocusing effects in ideal antennas by means of computer computations in hopes that this will lend insight into the problem.

Figs. 5 through 10 show patterns derived by the sidelobe method. A comparison of these patterns with those obtained by the gain criterion shows little difference, but the main lobe does seem to come out more symmetrical under the former method. The sidelobe focusing technique is described in some detail below in order to give an account of the major factors involved.

As indicated above, the proper focus was sought by a process of taking principal plane patterns, examining the patterns for sidelobe levels, and then moving the feed so as to improve the patterns in some regard. Feed movements were of two distinct types and were accomplished by separate means. Axial movements of the feed (in and out) were accomplished by varying the shims which fix the position of a reference plane on the receiver-feed system relative to a reference plane on the housing which supports the receiver-feed system. Transverse movements of the feed were accomplished by varying the lengths of the spars which support the feed by means of locknuts

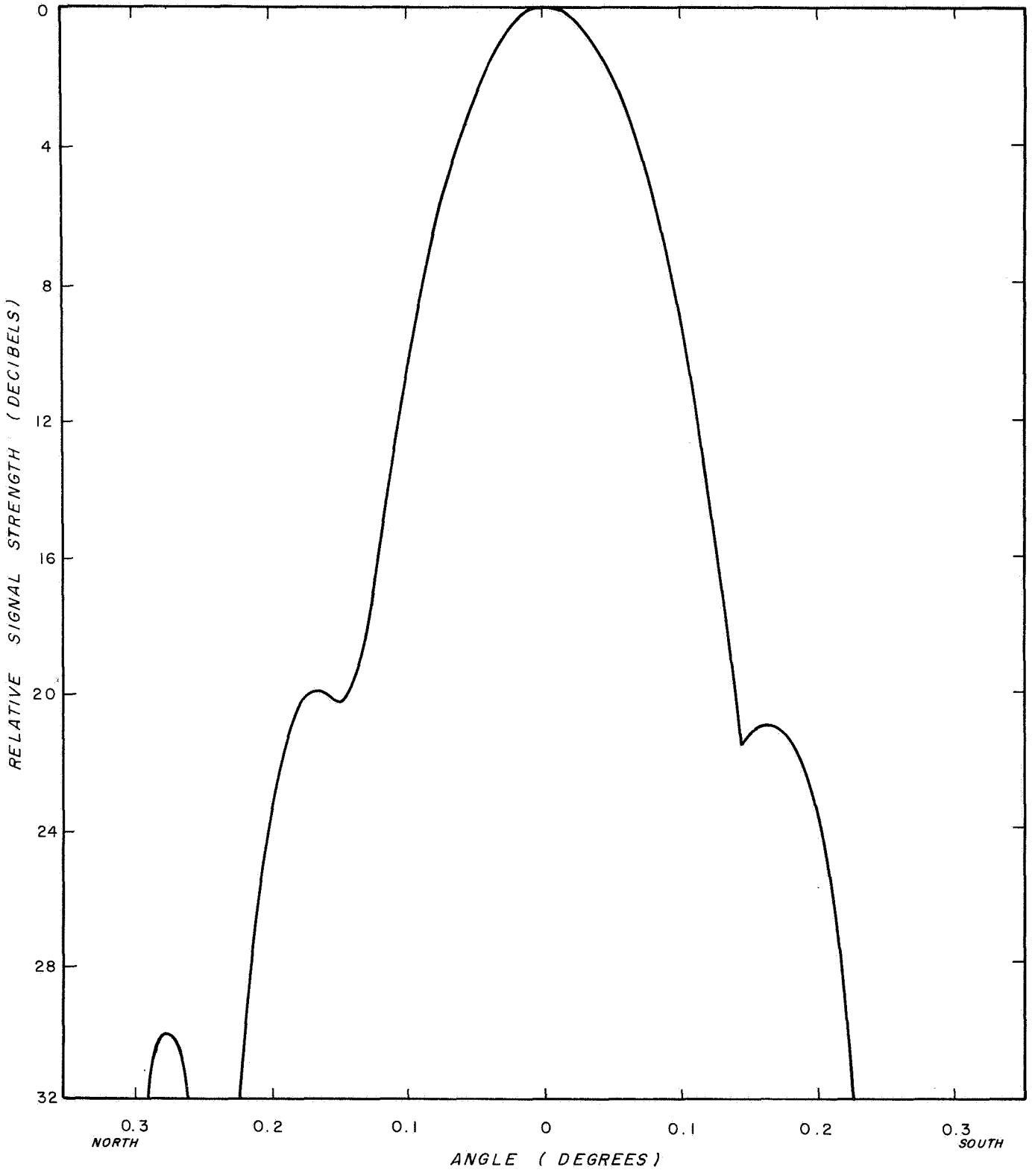

DECLINATION PATTERN AT 8.6 mm

Fig. 5.

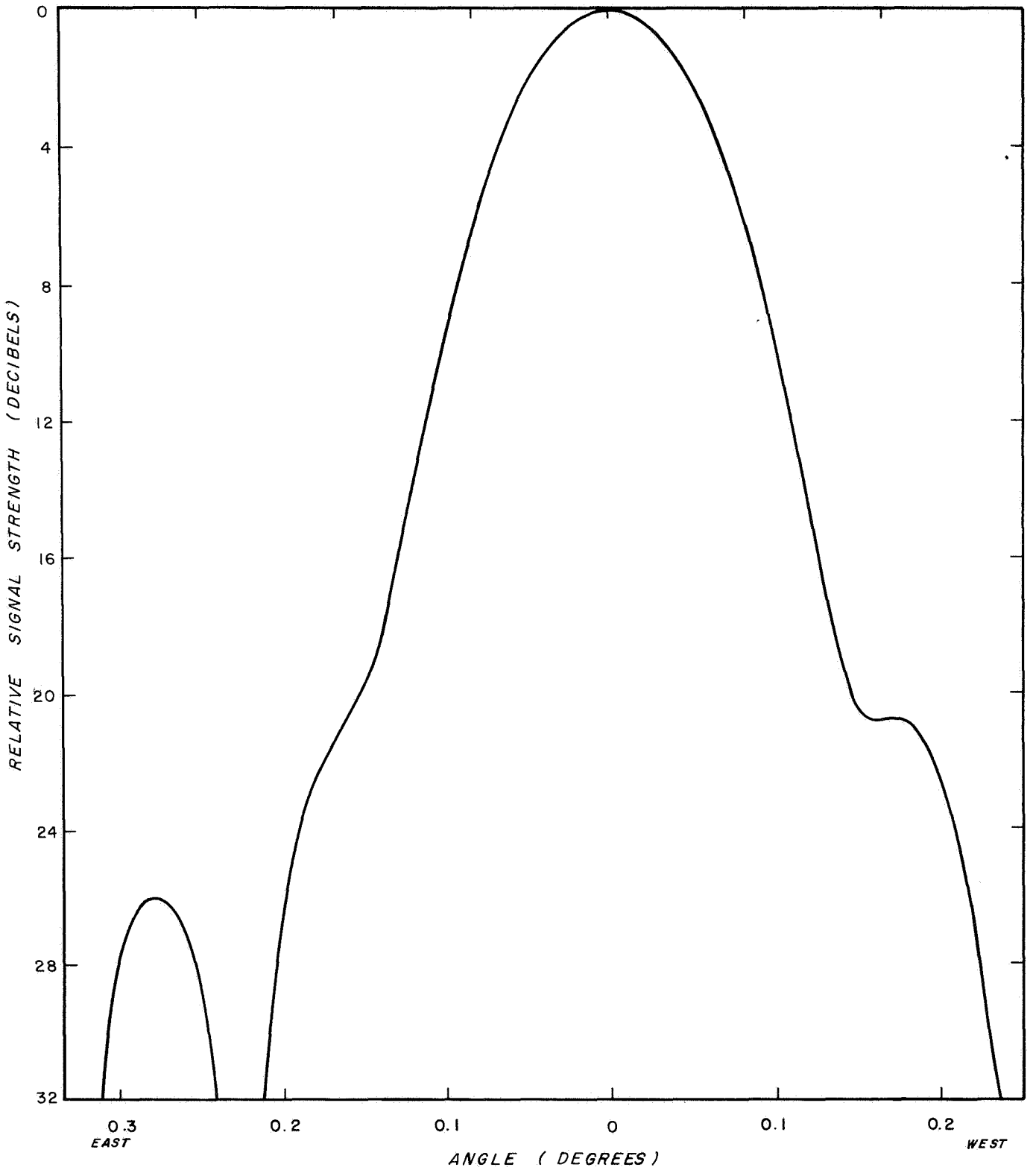

POLAR PATTERN AT 8.6 mm

Fig. 6.

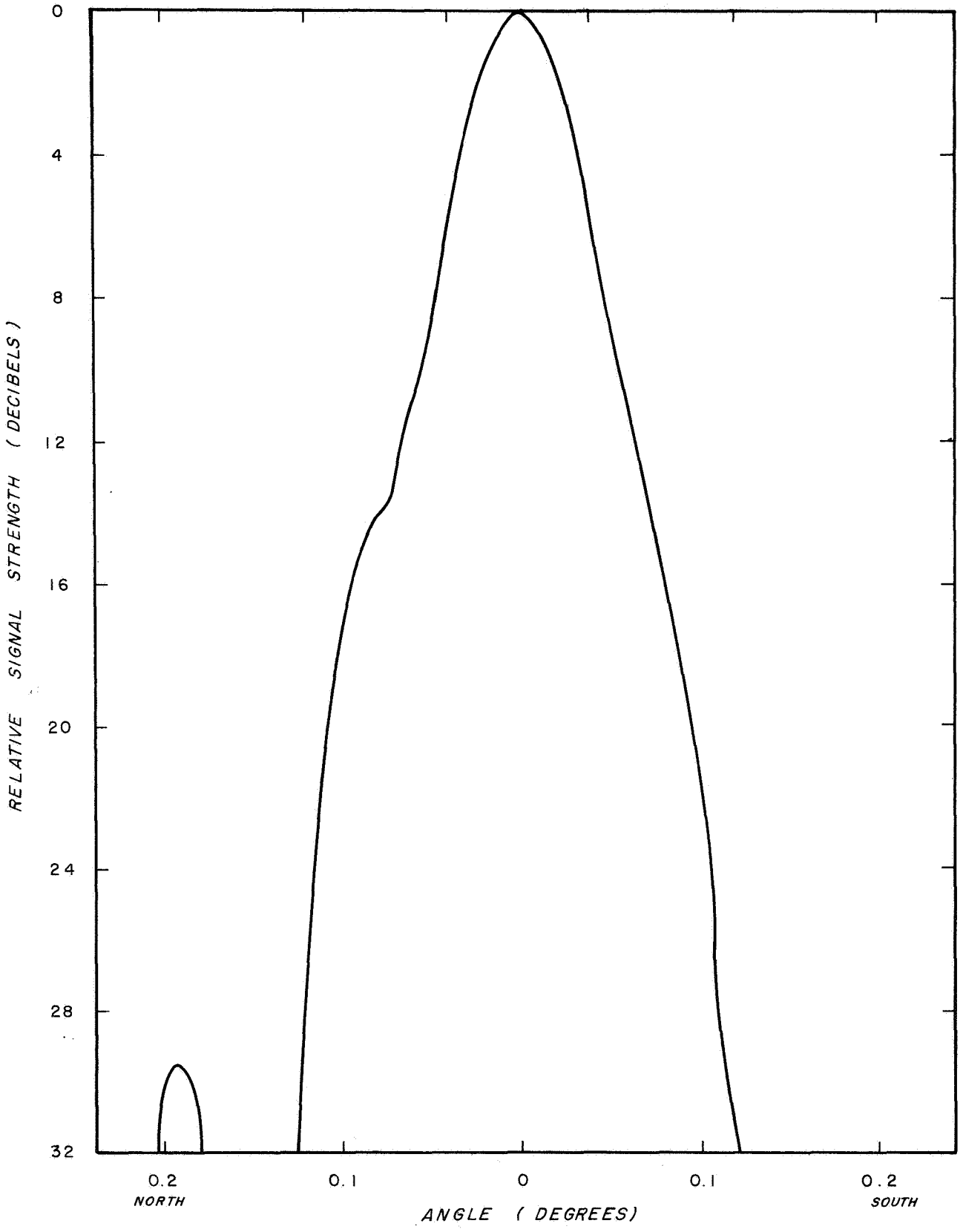

DECLINATION PATTERN AT 4.3 mm

Fig. 7.

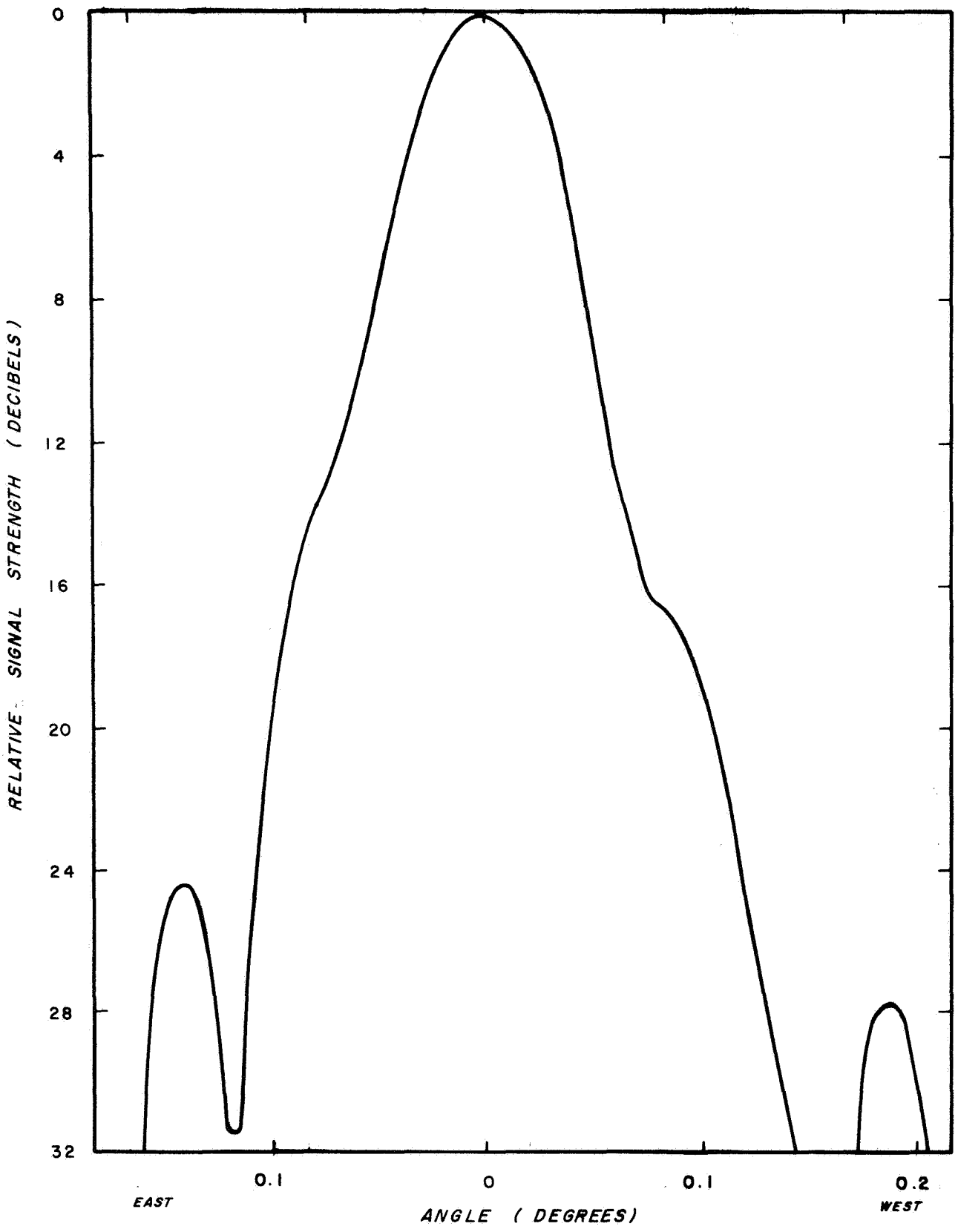

POLAR PATTERN AT 4.3 mm

Fig. 8.

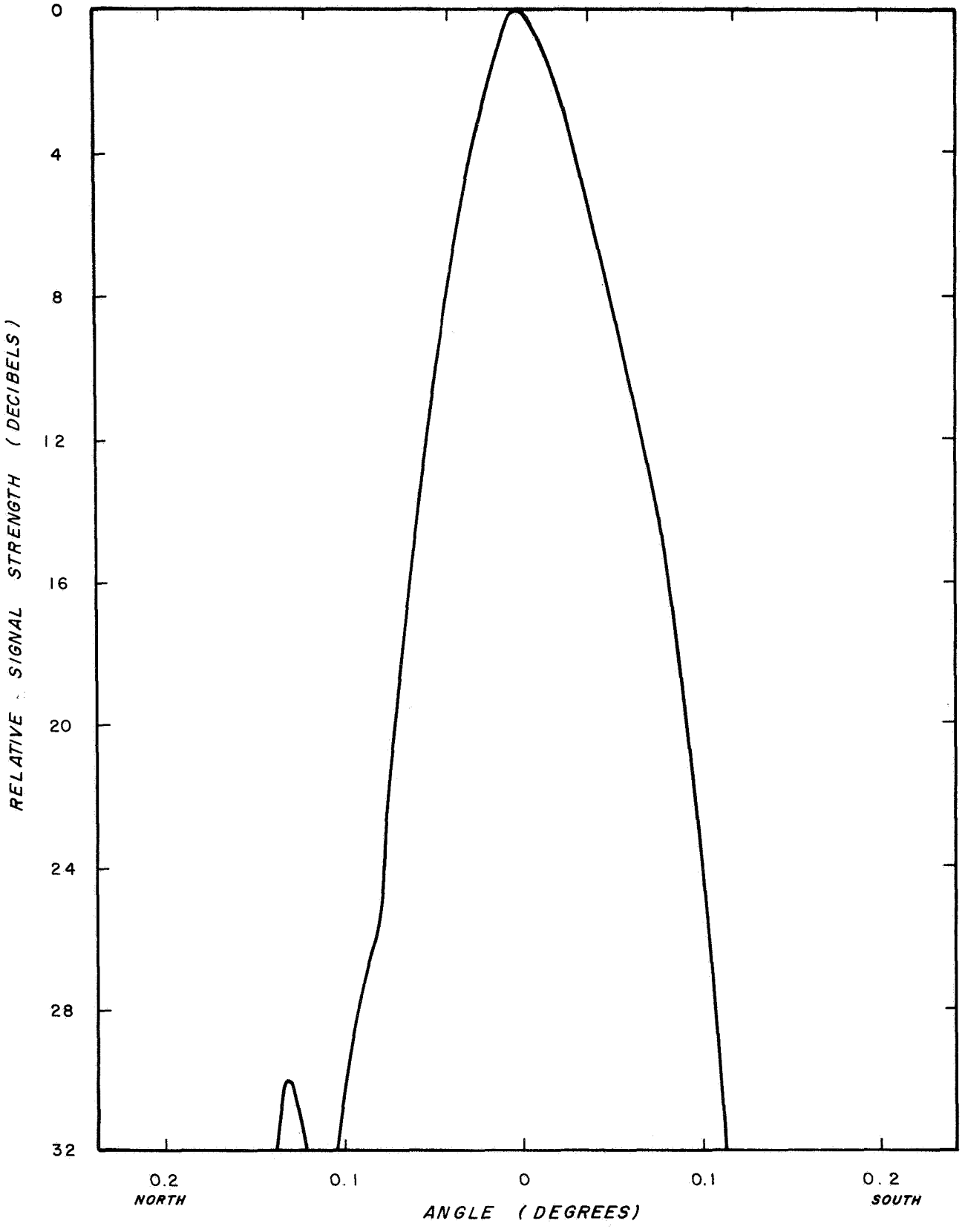

DECLINATION PATTERN AT 3.1 mm

Fig. 9.

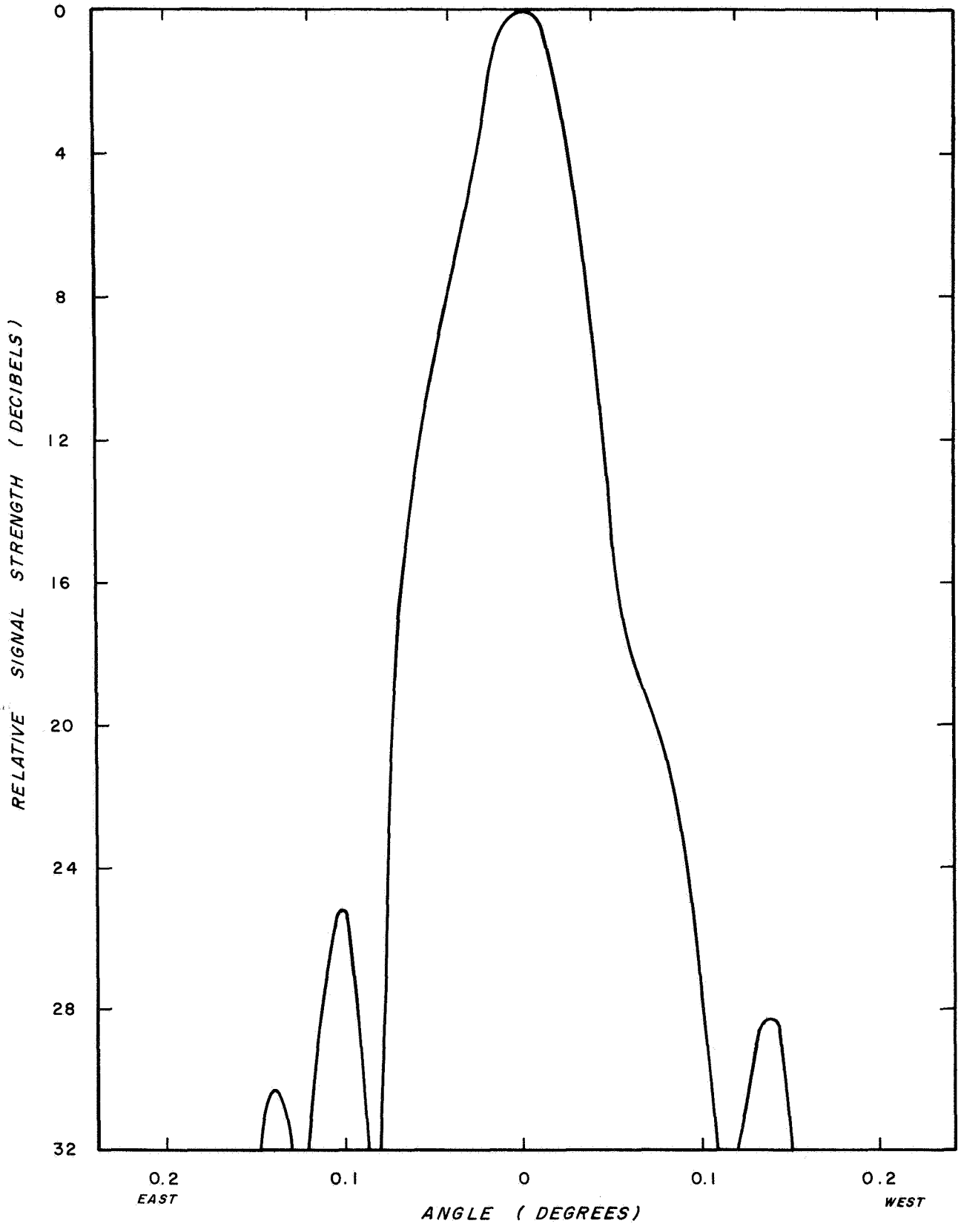

POLAR PATTERN AT 3.1 mm

Fig. 10.

provided for this purpose. Since these supports are located in the NW, NW, SW, and SE corners of the antenna, they had to be adjusted in pairs to produce the desired N-S and E-W motion. Furthermore, such motions affect the axial as well as the transverse position of the feed.

The method by which the correct feed position was sought and found is based on the following considerations. Transverse defocusing produces assymetric sidelobes, with the higher first sidelobe, the so-called coma lobe, on the true axis side of the main lobe. Since the feed position is also opposite the true axis from the main lobe, one must move the feed in a direction away from the higher sidelobe. For example, if in the N-S plane the higher first sidelobe appears south of the main lobe, then this indicates that the feed is too far south and should be moved north.

It was quickly found that for this antenna, axial focusing, i.e., moving the feed in and out along the axis of the antenna, varied the heights and structure of the first sidelobes. Specifically, moving the feed out from the reflector tended to make the polar (E-W) sidelobes small and distinct from the main lobe while the declination (N-S) sidelobe became large and tended to merge with the main lobe, which also broadened considerably. On the other hand, moving the feed in toward the reflector tended to have the opposite effect. The foregoing effects were found to be independent of the polarization of the incoming radiation and thus must depend upon the figure of the reflector. Here we see an indication that the focal distance

in the polar plane is greater than the focal distance in the declination plane. This is an important conclusion, which will be discussed in more detail later in this report.

B. Results

The focusing procedure using sidelobes which we have described is straightforward and one would expect that the proper focus would be quickly found. While this was our experience in one sense, in another sense it was not. In all, the feed was moved transversely thirty-four times during the focusing operation, twenty-four of these were used during focusing at 8.6 mm, four at 4.3 mm, and six at 3.2 mm. These numbers indicate only the number of times the feed was moved in the transverse plane; at most positions at least two axial positions were tried. In all, over one hundred feed locations were tried.

The large effort expended on focusing was a result of our dissatisfaction with the patterns obtained at first. Applying the method given above, we quickly obtained a focus satisfying our criterion - all four principal sidelobes were equal. However, the patterns so obtained were quite unsymmetric in the polar plane and this led to suspicions that something was wrong. Accordingly, a systematic search for a better focus was undertaken, during which the feed was moved systematically along the east-west direction in small increments. This process confirmed that the original focus was indeed the best obtainable.

Once the proper focus at 8.6 mm was found, the wavelength of measurement was changed to 4.3 mm and the process was repeated. This time only small feed movements were tried and a slight improvement was made. At 4.3 mm we had some difficulty distinguishing the sidelobe levels and thus had a little difficulty deciding on the optimum feed position.

The wavelength of measurement was then changed to 3.2 mm. Here we had very little success improving the focus. It was quite difficult to distinguish levels of the sidelobes, which were well merged with the main lobe (see Fig. 9 and 10). Furthermore, feed movements brought unexpected and unsystematic changes to the patterns. As time was short, the feed was placed at the optimum position obtained at 4.3 mm and the pattern and gain measurements reported in the next two sections of this report were made with the feed fixed at this position.

The procedure just described was followed during the summer of 1967, and the feed position so obtained was used during the winter and spring observations. During the summer of 1968, the other two focusing criteria were used and considerable time was again devoted to searching for the optimum focus, with disappointing results. In truth, our original conclusion, that the antenna has different focuses in the two principal planes, seems to be valid. This means that no ideal focus exists, i.e., one where the patterns resemble the theoretical patterns. Of course, some sort of optimum focus does exist, but this is hard to locate due to the general "fuzziness" of the focus.

Our recourse would seem to lie in developing an antenna feed which would have different phase centers in the two principal axes. This would be analogous to placing errors in the secondary mirror of an optical telescope to compensate for the errors in the primary mirror. This problem will be discussed later in this report.

IV. PATTERNS OF THE ANTENNA

A. Measurement Techniques

Patterns of the antenna were taken in the principle planes only. The method used was the usual one of moving the antenna at a constant angular velocity while at the same time recording the antenna position and power response on a chart recorder. For purposes of pattern taking the receiver was in logarithmic mode so that its response was approximately linear in decibels. The angle markings were taken directly from the antenna position indicating readouts and were marked on the chart simultaneously with the receiver response. Markings were made very 0.010° in both planes.

The chart was calibrated in decibels before and after each pattern by making known changes in the transmitted power. The chart was marked at 0, -3, -10, -15, -25, -30 decibels. Due to the limited range over which the receiver was approximately logarithmic, patterns had to be taken in two separate ranges: 0 to 15 dB and 15 to 30 dB. The calibration reference was derived from the precision r.f. attenuator in the transmitter. The transmitter circuit is shown in Fig. 4.

For these measurements, the receiver was arranged as in Fig. 2. In order to avoid the test signal's drifting out of the receiver passband, a modulation signal was applied to the transmitter klystron reflector. This modulates the transmitter frequency insuring that it will periodically sweep through the receiver passband. Thus the receiver output is a series of pulses. This signal is peak detected and the resulting "d. c." signal is fed back to the i. f. amplifier circuit, thus producing an approximately logarthmic response character to the entire receiver.

B. Results

1. Patterns at 8. 6 mm

The patterns obtained by the sidelobe criterion at 8. 6 mm are shown in Figs. 5 and 6. The half-power beamwidths are 0. 114° and 0. 119° in the declination and polar planes, respectively. As can be seen the first sidelobe level is approximately 20. 5 dB below the peak of the beam. The sidelobes are partly merged with the main lobe, particularly the east sidelobe in the polar pattern, but the sidelobe levels are easily distinguished. It might be noted that the declination pattern is fairly symmetric, while the sidelobe structure in polar is somewhat unsymmetrical. The patterns obtained by the sidelobe criterion were satisfactory, so the gain criterion was not used at this frequency.

2. Patterns at 4. 3 mm

The patterns obtained at 4. 3 mm by the sidelobe method are shown in Figs. 7 and 8. The half-power beamwidths are 0. 059° and 0. 060°

in the declination and polar planes, respectively. The sidelobes are merged with the main lobe and the proper sidelobe levels are difficult to distinguish. The average sidelobe level might be estimated as 15 dB. The lack of symmetry is evident and indicates that a slightly better feed position might exist.

Patterns obtained by the gain method did not differ greatly from those shown, except that the beamwidths changed somewhat. Specifically, the declination and polar beamwidths were found to be .069° and .066°, respectively.

3. Patterns at 3.1 mm

The patterns obtained at 3.1 mm by the sidelobe method are shown in Figs. 9 and 10. The half-power beamwidths are 0.049° and 0.048° in the declination and polar planes, respectively. The sidelobes are well merged with the main lobe and the sidelobe levels are very difficult to estimate. Our guess would be 10-12 dB.

Patterns obtained by the gain method differed little from those shown, except again for the beamwidths. At this frequency, focusing for maximum gain resulted in beamwidths of .046 and .054 in the declination and polar planes, respectively.

4. About Polarization

Patterns were taken in both horizontal and vertical polarization. We call the polarization "horizontal" when the received electrical field vector is aligned with the declination circles on the celestial sphere, i.e.,

is perpendicular to the polar axis. Vertical polarization is orthagonal to horizontal polarization.

The patterns were found to vary only in minor detail between the two polarizations. The feed design would therefore seem to be optimum and the characteristics of the patterns are determined by the figure of the antenna. For this reason we have not shown both sets of patterns and have labeled the patterns "declination" and "polar" rather than E- and H-plane as is customary.

V. GAIN MEASUREMENTS

A. Measurement Techniques

The gain of the antenna was measured by comparing its effective area with that of a calibrated horn antenna. The comparison was accomplished by varying the transmitted power until the received power from the two antennas were equal, it being understood that the comparison of received powers was sequential and not simultaneous. The transmitted power was varied for comparison purposes with a calibrated precision attenuator. The method chosen for this measurement (r.f. attenuation) is felt to be the most accurate of the several available because one need not assume mixer linearity or worry about the system noise changing the operating point on the peak detector.

Since attenuator setting differences of 35-40 dB are required for this measurement, attenuator accuracy is a crucial factor in determining the overall accuracy of the measurement. Also, the gain of the conical horn is

equally crucial to the overall accuracy. The methods of horn calibration are discussed in Appendix A and B.

The accuracy of these measurements is difficult to state quantitatively. All errors tend to be systematic, so repetition of measurements does not increase accuracy. The best one can do in this situation is to make the measurements by as many different methods as possible and then make an average, possibly using subjective confidence factors. This we have sought to do, although our program is incomplete at present. At present, the best statement we can make is that attenuator readings are felt to be accurate to ±.2 dB (4%), but that horn gain values are not so well known. An overall gain accuracy of ±0.5 dB (10%) would be a pessimistic guess.

B. Results

The following table summarizes the gain measurements made to date.

Freq. (GHz)	Horn Gain (dB/iso.)	Atten. (dB)	16-Foot Gain	Eff.
35.0	28.6[1]	34.3	62.9	61%
69.75	32.0[2]	36.6	68.6	58%
95.0	31.2[3]	38.8	70.0	44%

Sources of Horn Gain Values:

(1) The value 28.6 dB for the 8 mm horn comes from a calculation (See App. A). The horn gain is due to be measured.

(2) The 32.0 dB gain for the 4.3 mm horn is a measured value. We calculate a value 31.9 dB, which indicates an efficiency of 57%.

(3) The horn gain of 31.2 dB/isotropic for the horn at 95.0 GHz is based upon a recent measurement at this laboratory in which the author of this report did not participate. We calculate a value of 33.7 dB, which indicates an efficiency of 78%, much too high.

C. Astronomical Evaluation of Gain

One measurement has been made on the antenna which bears on the gain question. In the spring of 1967, Jupiter was measured at a frequency of 35.0 GHz. If the value of Jupiter's disk temperature is assumed to be 152°K, as theory and some measurements indicate[6-8], then the efficiency of the antenna computes to be 55%. On the other hand, if the value of 112°K is assumed[3], the efficiency comes out 74%.

VI. STABILITY OF THE ANTENNA

A. Experiment Performed

As mentioned in the Introduction of this report, a knowledge of the stability of electromagnetic properties of an antenna is requisite to its use. This is true because the antenna must frequently be used under conditions somewhat less ideal than those under which it was calibrated. For example, most of the work reported in the present document was performed under night-time conditions, whereas many observational events, e.g., solar

observations and Venus observations near conjunction, must inherently be performed in daytime.

On 10 August 1967 an experiment was performed in order to determine the effects of solar heating on the antenna's properties at 8.6 mm wavelength. Measurements of the antenna's gain, pattern and boresight angle were made every hour from 0600 hrs (CDT, predawn) until 1900 hrs. At the beginning of this period the antenna was in thermal equilibrium. At about 0730 hrs, the sun began to strike the face of the antenna, and by 1100 hrs the entire face of the antenna was in direct sunlight. Thus, during the morning the antenna surface was subjected to differential heating and the effects of thermal expansion would be expected to degrade antenna performance. At approximately 1300 hrs the backup structure of the antenna began to experience direct sunlight, though from a varying direction as time progressed. At approximately 1500 hrs the shadows of the astrodome was falling upon the back of the antenna, again leading to differential heating and by 1800 the entire antenna was in the shade. Thereafter the sunlight could not strike the antenna.

Thus we see that twice during the day the antenna was subjected to differential heating, once on its face and once on its back. This represents an extreme in environmental effects and such severe conditions would rarely be encountered in astronomical observations.

B. Results

Fig. 11 shows the gain, the boresight direction, and the principal plane beamwidths of the antenna at 8.6 mm wavelength, plotted versus time of day. The condition of the antenna relative to the sunlight is marked below the abscissa for ease of reference.

The effects of differential heating are easily noticed. During both such periods the gain dropped and the beamwidths increased. This clearly is the effect of distortion of the antenna figure due to thermal expansions. Of interest is the remarkable stability of the boresight direction throughout the period of the experiment. All deviations are less than 0.007° from the mean value, and this is less than 10% of the beamwidth at this wavelength. This indicates that the pointing properties of the antenna are sufficiently stable for operation under all conditions. In general, the experiment indicates that the antenna is usable at 8.6 mm wavelength under all reasonable conditions. At higher frequencies the properties of the antenna would be more sensitive to environmental effects.

VII. POINTING ACCURACY OF THE ANTENNA

A. Nature of the Problem

The antenna is equipped with readouts which indicate the declination and hour angle at which it is pointed. These angles are derived from encoders which measure the relative angles of the antenna mount axes. There are several effects which would cause the actual electromagnetic axis of the

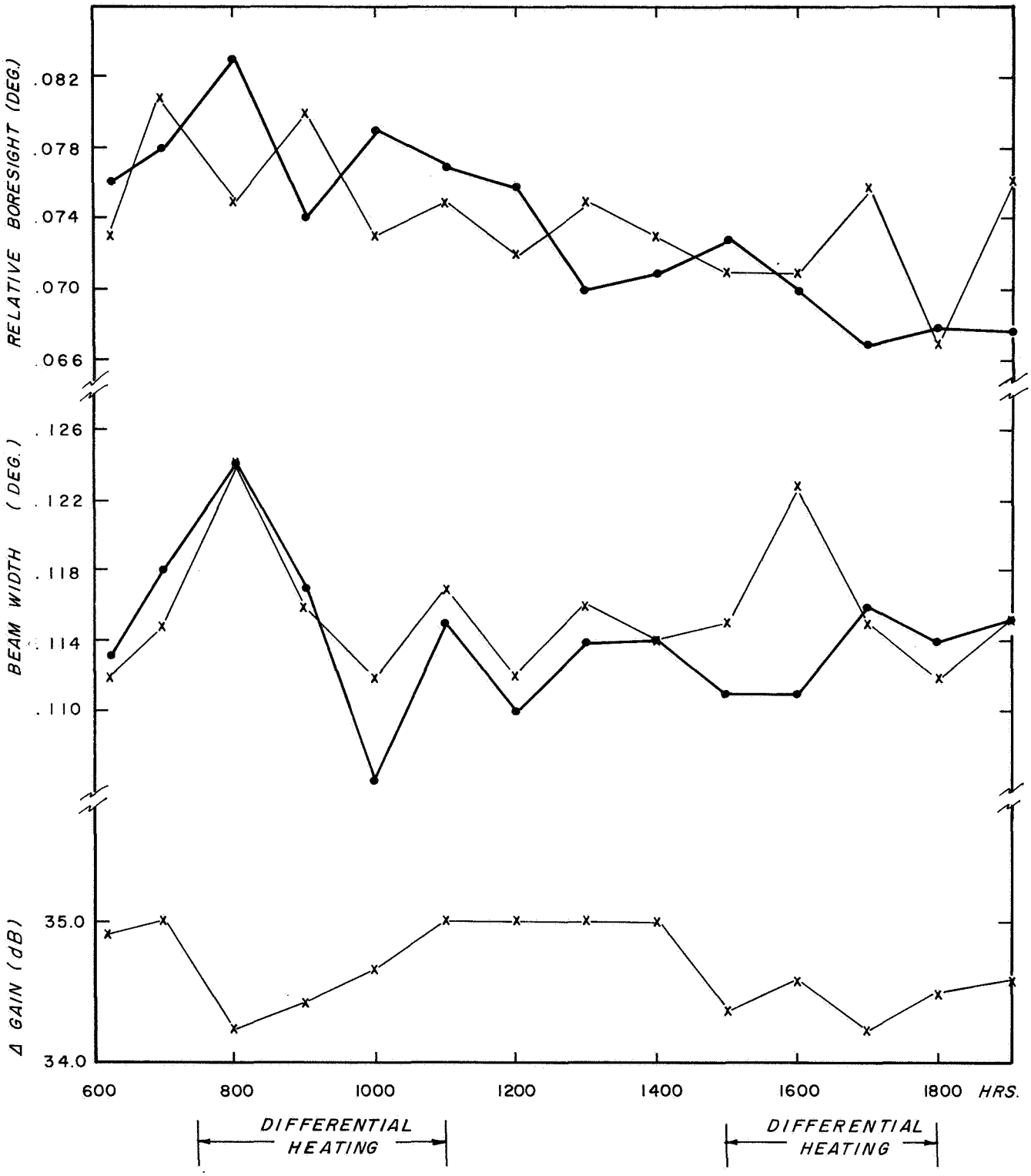

ANTENNA STABILITY TEST

Fig. 11.

antenna to differ from the position indicated by the readouts. These effects include:

1. Polar Axis Tilt. If the polar axis of the antenna were not aligned with the earth's axis of rotation, errors would result, primarily in the declination coordinate.

2. Declination Axis Non-orthogonality. If the declination axis were not orthogonal to the polar axis, hour angle errors would result.

3. Sag. The sag of the feed due to gravity would depend on the zenith angle and would yield errors in both coordinates.

4. Refraction. Refraction would cause errors in the apparent zenith angle of arrival and would contribute to errors in both coordinates.

B. Polar Axis Tilt Evaluation

The magnitude and direction of the polar axis tilt were measured through use of the optical telescopes which are rigidly mounted on the antenna mount structure. In this experiment, we measured the indicated declination of a number of stars as a function of hour angle. A simple analysis indicates that, after refraction is accounted for, the declination errors should obey an equation of the form

$$\Delta\delta = K_1 + K_2 \cos (t - \varphi).$$

where

$\Delta\delta$ = declination error

K_1 = additive constant of little importance

K_2 = magnitude of polar axis misalignment

φ = direction of polar axis misalignment.

The data are shown in Fig. 12. When the parametric equation is fitted to the data in a least-mean-square sense, axis tilts of $K_2 = .078°$ and $\varphi = -27.6°$ were determined. The smooth curve in Fig. 10 shows the degree of fit of the equation, the residual rms error being .0010. The magnitude of the tilt error seems large, but adjustments can be made on the mount to correct this tilt.

C. Sag Evaluation

The feed sag was evaluated by comparing solar limb crossings as indicated by optical and radiometric means. The method involves doing drift scans on the sun as it rises and marking the optical limb crossings as indicated by the optical telescopes. Assuming no difference in optical and radio refraction, one reasons that sag errors in hour angle are given by the following equation:

$$\Delta T = K_3 + K_4 \sin\theta \sin\mu$$

where

ΔT = difference in apparent hour angle of optical and radio axes

K_3 = offset constant of little importance

K_4 = total sag, zenith-to-horizon

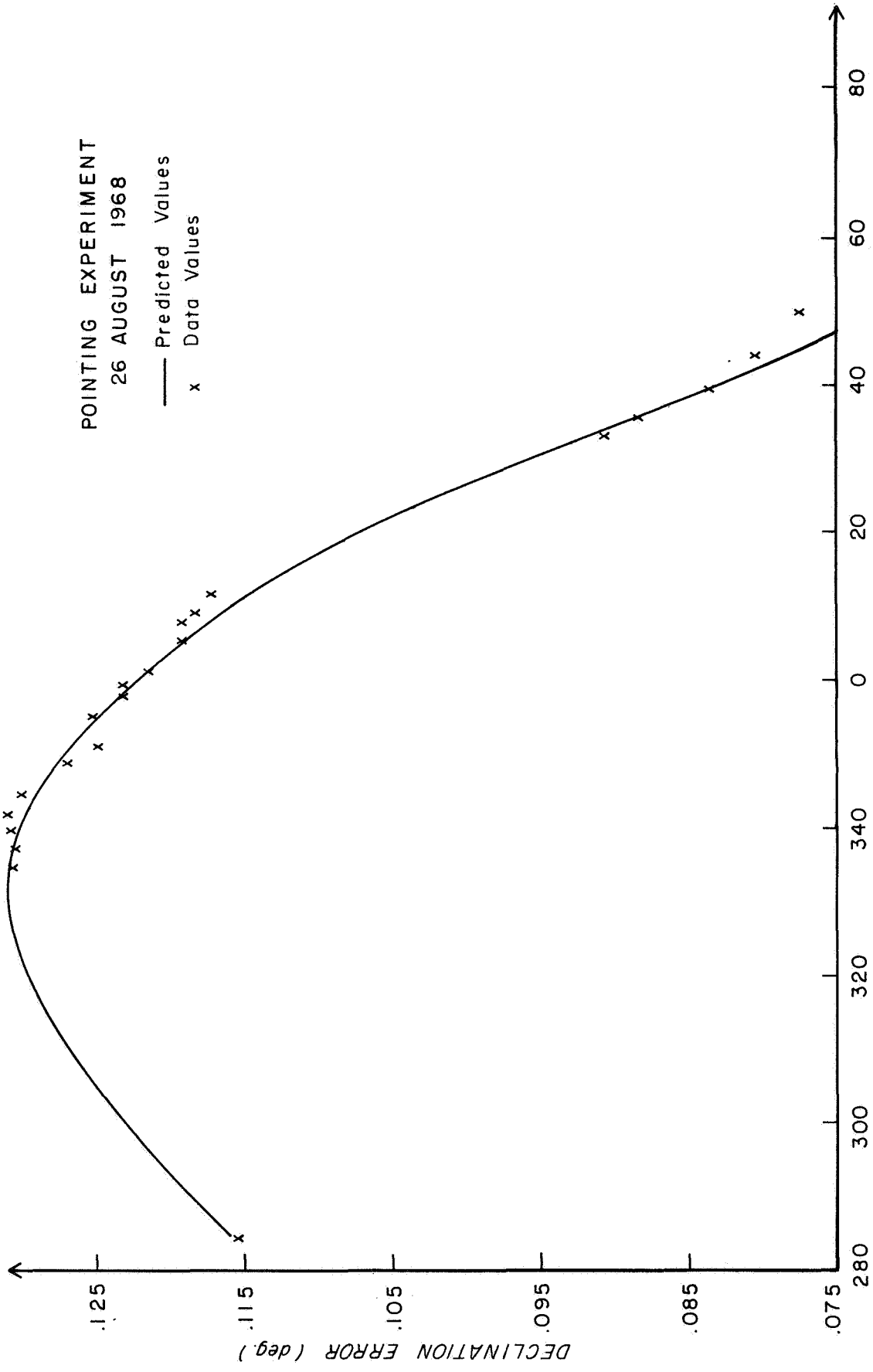

DECLINATION POINTING ERRORS

Fig. 12.

θ = zenith angle

μ = angle between hour angle circle and meridian circle, negative before transit.

The parametric equation was fitted to the data and sag was determined to be $K_4 = .015°$. Fit was quite good with an r.m.s. error of .002°.

The experiment was performed again with different counterbalance weights on the feed, but the data have not been analysed as yet. Once the second experiment is evaluated, it should be possible to compute the proper counterbalancing to reduce the sag error to a negligible amount.

D. Summary

The pointing accuracy of the antenna is not yet determined because the declination axis non-orthogonality has not been measured. An experiment to accomplish this is in the planning stages.

The errors which have been evaluated are certainly significant in comparison with the antenna beamwidth of 0.050° at 3.2 mm. However, the errors fit simple models quite well and in principle can be corrected if warranted.

VIII. SITE EVALUATION

The decision to move the radio telescope from Austin to Mt. Locke was motivated by a desire to benefit from the superior astronomical climate of the latter site and involved certain logistics problems. After use of the Mt. Locke site for a period of one and one-half years, it is perhaps apropos to discuss our current evaluation of the site.

A. Weather Patterns

According to residents, the past year or so has been abnormally rainy in the Davis Mountains, but the general weather patterns are easily discerned. During the summer months the period from midnight to noon is generally clear and ideal for observations. Afternoons, on the other hand, tend to be cloudy and rainy and unsuitable for observations. These conditions hindered the calibration work until we shifted our work to the morning hours, after which very little time was lost.

During the remainder of the year, the weather was ideal for observing except when large frontal systems move through. On the average, the site has proven up to expectations with regard to weather.

B. Attenuation Studies

One of the principle advantages of the Mt. Locke location is its high altitude, placing the antenna above approximately one-half the earth's atmosphere. Nevertheless, atmospheric attenuation is still a significant factor, particularly at the shorter wavelengths, and a measurements program has been initiated which will allow the absorption to be estimated at anytime. The approach taken is semi-empirical, and consists of simultaneously measuring the atmospheric loss and the absolute humidity at the site. The former measurement uses the sun as it rises or sets; the latter measurement is made with a sling psychrometer. Since the absorption is due principally to oxygen (a stable constituent of the atmosphere) and water vapor

(a variable constituent), one would intuit a strong correlation between opacity and absolute humidity at the site, particularly if good observing conditions prevail.

Assuming a flat earth, one would expect the antenna temperature due to a radio source to vary with zenith angle according to the relation:

$$T_a(\theta) = T_s\, e^{-\tau \sec \theta}$$

where

T_a = antenna temperature

T_s = source temperature

τ = zenith opacity

θ = zenith angle

Thus when one plots $\ell n\, T_a$ vs sec θ, the slope would be the opacity τ. Fig. 13 shows a typical day's data, plotted in this fashion. On this particular day, the zenith opacity was 0.64 dB and the absolute humidity was 4.48 gm/cu.ft.

During the summer of 1968, data of the type given above was taken at 8.6 mm, 4.3 mm, and 3.2 mm. The data at λ = 3.2 mm is shown in Fig. 14. The expected trend is clearly evident, but the data points are too few to base quantitative conclusions on. The range of humidity values does not vary greatly during the summer months and wintertime readings are needed before a regression analysis can be applied. It is significant

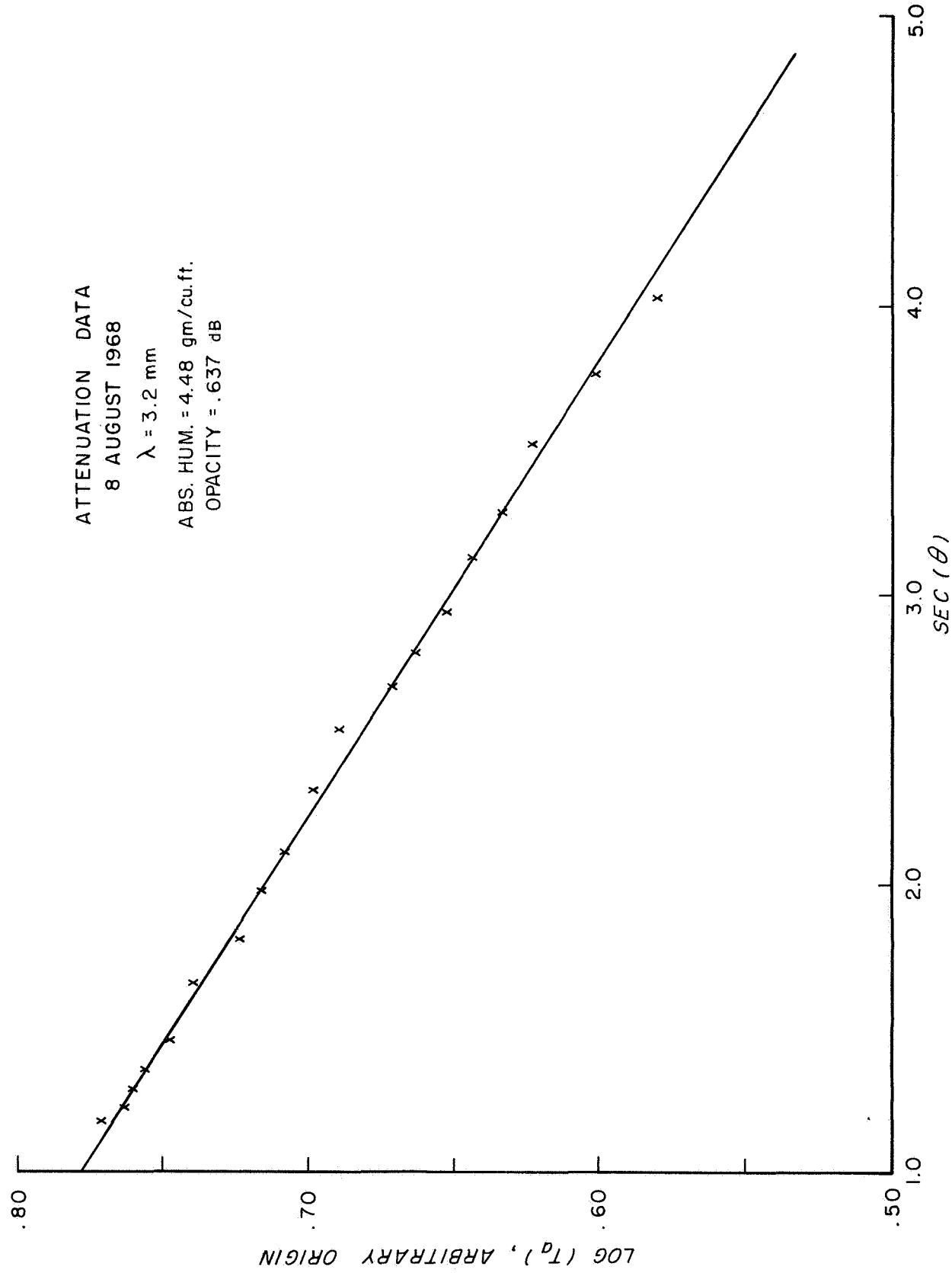

OPACITY DATA
Fig. 13.

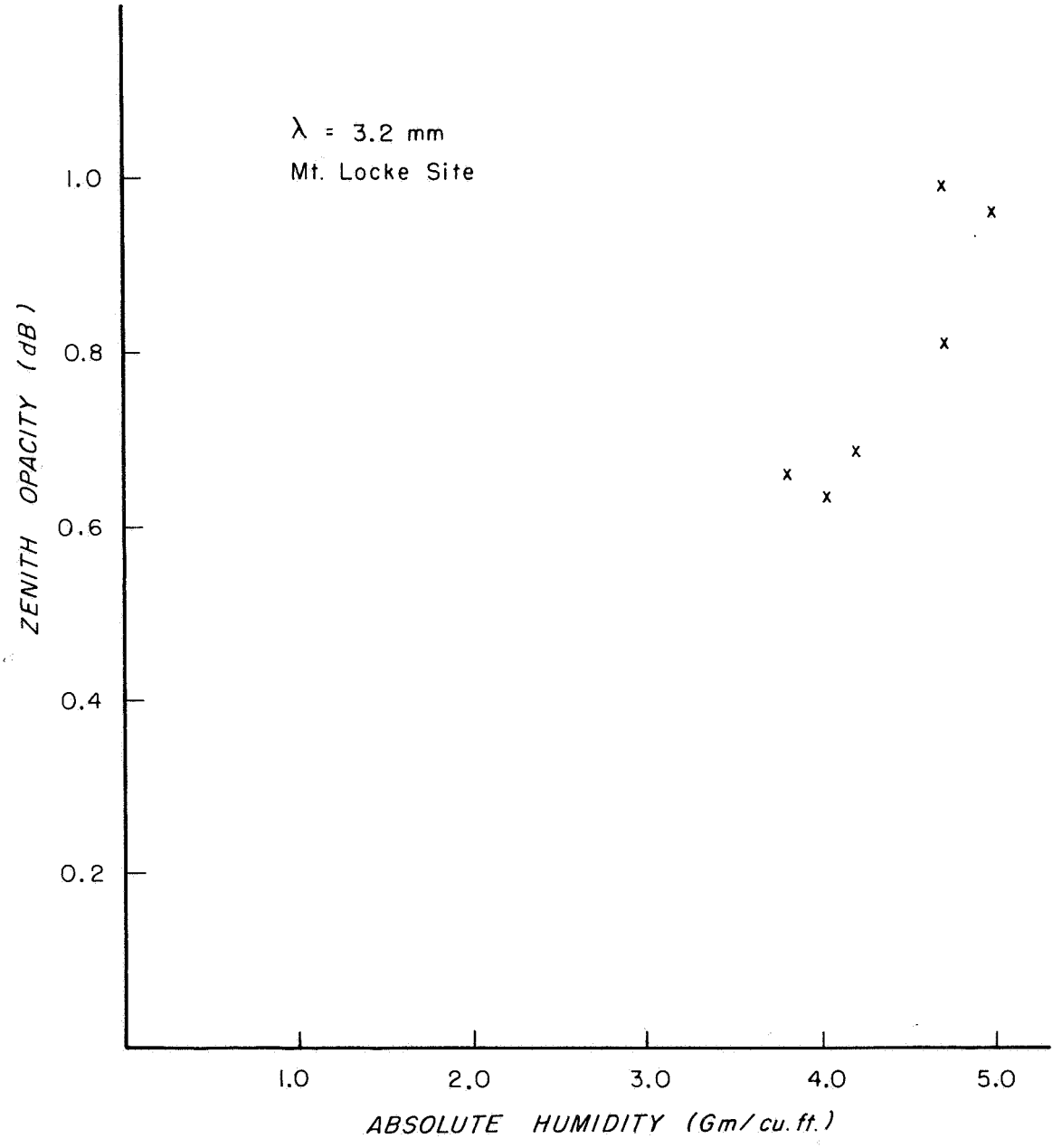

ZENITH OPACITY VS. ABSOLUTE HUMIDITY

Fig. 14.

that the values of opacity shown are approximately one-half those typical of Austin under the same conditions.

IX. FUTURE ANTENNA CALIBRATION WORK

Through this report we have stressed the fact that the calibration of the 16-foot radio telescope is incomplete. Most of the work discussed represents the beginning of our measurement program. There are, in addition, at least two areas in which work must be initiated in the future. These we discuss briefly in the present section.

A. Feed Design

When discussing the focusing procedures, we made mention of the fact that the antenna seemed to have different foci in the two principal planes. This was indicated by the fact that if the feed was at one focus, the declination pattern was near ideal but the polar pattern was plainly defocused. On the other hand, if the feed was moved out by approximately 0.1 inches, the polar pattern became ideal and the declination pattern was defocused. This behavior was independent of the polarization, i.e., feed orientation, and hence must originate in the figure of the antenna. These facts indicate that the antenna has focal lengths in the principal planes which differ by approximately 0.1 inch. There is no evidence that the foci are not coaxial.

Our current ambition is to design a feed which will compensate for this effect. Normally an antenna feed is designed to have one phase center, i.e., to radiate a wave whose constant phase surfaces are spherical.

We would seem to require a feed with different phase centers in the principal planes. Such a feed would radiate a wave whose constant phase surface is ellipsoidal. This technique is the radio analog of the optical technique of placing deliberate errors in the secondary mirror of the telescope so as to compensate for the errors in the primary mirror.

B. Calibration at 140 GHz

The precision with which the antenna was constructed should allow operation at the 140 GHz window. That is, the small scale surface deviations should be small enough to allow a diffraction pattern to be formed. On the other hand, if the average figure departs from a paraboloid of revolution, as suggested in the preceeding section, then this effect would be more destructive to the antenna properties at the higher frequency. In that event, a smaller, interior sector would surely be useful.

We have the necessary transmitter and receiver to calibrate the antenna at 140 GHz. This will probably be attempted during the coming spring months. Should the antenna prove useful, we have the necessary equipment to place it into operation as a radio telescope in this window where it has few if any competitors.

Interest in establishing the highest useful frequency has been generated by Dr. Bruce Ulrich of the Astronomy Department. Dr. Ulrich is developing supercooled detectors utilizing the Josephson effect at 2 mm and 1 mm. Such detectors have potential application on the 16-foot antenna.

Granted success at the 2 mm (140 GHz) band, calibration at the higher shorter wavelength would be attempted through astronomical observations. This work will not be initiated in the near future.

Appendix A

Horn Gain Calculation

The gain of the conical reference horn enters directly and crucially into the measurement of the gain of the 16-foot antenna. We have sought both to derive and measure the gain of the horns we use, with results which agree significantly. The purpose of this Appendix and the next is to present the methods used in determining the horn gain.

A1. Assumptions Underlying Calculation. The horn is conical, with a transition section to convert smoothly from rectangular waveguide to a circular cross-section. The rectangular waveguide section supports only the dominant mode but the horn beyond the transition section can support a large number of modes. We assume that these higher order modes are not excited. Furthermore, we assume that all the energy in the dominant TE_{01} mode in the rectangular waveguide is converted to the dominant mode of the horn.

The conical horn can be thought of as a spherical waveguide and presents an analytical problem which is tractable though formidable. Clearly the fields in the horn are essentially those in a circular TE_{11} mode since the horn angle is so small (approximately 8°). The principal effect of the flare would be to produce a curvature to the field lines and constant phase surfaces to be spherical with a center of expansion located at the apex of the cone. In the analysis of the horn, the fields are

assumed to be as described above. Actually, in the calculation of the on axis gain, the slight curvature of the field lines at the horn aperture would have only a small effect on the final result since the horn angle is so small and the fields are weakest near the edge of the aperture where the angle is maximum. We have therefore chosen to ignore the curvature of the field lines and retain only the effects of the spherical constant phase surface. Thus, in the gain calculation, the field lines are assumed to lie in the aperture plane of the horn and to be those of the TE_{11} mode in circular waveguide, except that a quadratic phase term is included to account for the spherical constant-phase surface.

At the aperture plane, free-space spherical waves will be launched from the waves of the waveguide mode. We assume that negligible reflection takes place at the horn mouth, based on the large aperture. In Marcuvitz[9], calculations for similar circumstances indicate negligible reflections.

A final assumption, and the weakest one, is that the effects of currents on the exterior of the horn are negligible. In other words the aperture field method[10] will be used to compute the gain of the horn. This assumption is made because otherwise the problem is intractable. In Silver[10] in a number of places comparisons are made between calculated and measured parameters with substantial (though not spectacular) agreement, thus validating this approach to a degree.

A2. Basic Gain Calculation. The problem which we have framed is essentially that of a circular waveguide radiating into free space with a quadratic phase error. This problem, without the phase correction term, has been solved by Chu[11] and is summarized nicely by Silver[12]. We chose to quote Chu's result and then made a correction for the phase error.

Following Silver, we write the radiation pattern as

$$N(\bar{a}_r) = \int_{\text{Aperture}} \bar{E}_t(\bar{r}')_e^{-j\varphi_o\left(\frac{r'}{r_o}\right)^2} e^{jk\bar{a}_r \bar{r}'} \, d(\text{area}')$$

where

$N(\bar{a}_r)$ = radiation vector in $\bar{a}_r$ direction

$\bar{r}'$ = coordinant in aperture plane

$E_t(\bar{r}')$ = aperture field, without phase error (TE_{11} mode)

φ_o = maximum phase error, to be discussed in the following section

r' = cylindrical radial coordinant in aperture plane

r_o = radius of aperture

$k = \frac{2\pi}{\lambda}$

Taking the polarization into account, substituting the fields of the TE_{11} mode, integrating in cylindrical angle, and setting $\bar{a}_r \bar{r}' = 0$(on axis), one reduces the equation to:

$$N_x = K \int_0^{r_o} J_o\left(\frac{1.841}{r_o} r'\right) e^{-j \varphi_o \left(\frac{r'}{r_o}\right)^2} r' dr'$$

K = a constant

The preceeding is used by Silver with $\varphi_o = 0$ to compute the on axis gain. The result he derives for negligible reflection at aperture is:

$$G_o = 33.0 \left(\frac{r_o}{\lambda}\right)^2 \text{ dB/isotropic}$$

We chose to take the phase error into account by introducing a phase correction term

$$G = G_o \Phi$$

where

$$\Phi = \left| \frac{\int_0^{r_o} J_o\left(\frac{1.841\, r'}{r_o}\right) e^{-j \varphi_o \left(\frac{r'}{r_o}\right)^2} r' dr'}{\int_0^{r_o} J_o\left(\frac{1.841\, r'}{r_o}\right) r' dr'} \right|^2$$

This method uses the published results maximally and is self-normalizing.

A3. Phase Correction. The parameter φ_o is the phase difference between the fields at the center of the aperture and those at the edge as seen from the axis of the horn. If the fields at a finite distance are of importance, the parameter φ_o will depend upon the distance from the aperture at which the

field (or gain) is evaluated. In other words, if one is not in the Fraunhofer or far-field region of the aperture, the phase error will depend upon where along the axis of the horn one desires to know the gain. In the present instance, the 16-foot antenna gain measurement definitely uses the Fraunhofer gain, but the gain measurement procedure described in the next Appendix uses the near-field region.

Thus, we chose to include phase curvature and near-field effects in evaluating φ_o. Simple geometry shows that:

$$\varphi_o = \pi \left(\frac{1}{\lambda_g L} + \frac{1}{\lambda_o R} \right) r_o^2$$

where

φ_o = maximum phase error in radians

λ_o = free space wavelength

λ_g = guide wavelength at horn mouth, assumed to be approximately λ_o

L = length of horn along side

R = distance from horn aperture to point of measurement

See Fig. 15 for the geometry.

The phase correction term, Φ, was computed for the wavelengths, horn sizes, and near-field distances relevant to the gain tests.

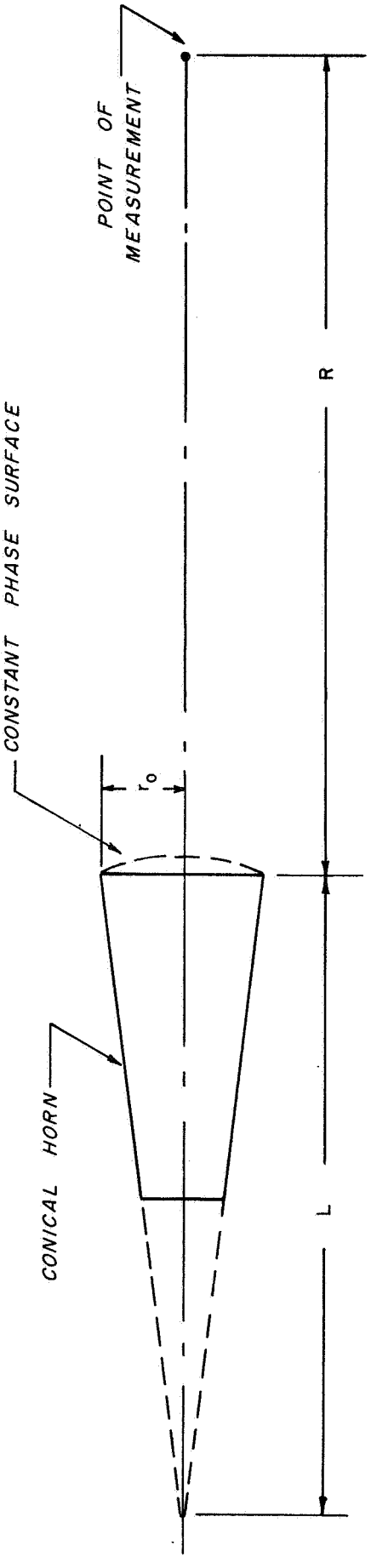

CONICAL HORN

Fig. 15.

Some of these results are presented in the next Appendix. The phase correction term ranged from .3 dB to 2.0 dB in the calculations.

A4. Loss of Horn Antenna. Owing to the method in which calibrations are made during observations on the 16-foot antenna, gain measurements are conveniently referred to the output flange of the horn antenna. For this reason, the gain computed at the aperture must be reduced by the absorption from the horn aperture to the output flange. This absorption has been computed approximately based upon the absorption formulas for circular waveguide, taking account of the changing radius of the "waveguide". The results of such a computation is approximately .05 dB, so it is a minor correction.

A5. Results. The results of the calculations described in this Appendix are summarized in the following table.

Wavelength mm	Horn Radius cm	Basic Gain dB/iso.	Phase Loss dB	Absorption dB	Calc. Gain dB/iso.
8.6	6.500	28.94	.30	.04	28.60
4.3	5.050	32.79	.84	.06	31.89
3.16	5.050	35.47	1.74	.07	33.66

Appendix B

Horn Gain Measurements

B1. Introduction. The calculated values of horn gain are being compared with laboratory measurements of the horn gains. This program is not complete but some results have been obtained. The basic method of measurement and the results which have been achieved will be presented in the present section.

Our present goal is to measure the horn gains at all the primary calibration frequencies (35, 70, 95, and eventually 140 GHz). Thus the antenna gain measurements will be based upon measured rather than calculated values of horn gain. The calculations have been performed to check the theory and to given interpolative ability. This is also a problem of inherent and widespread interest due to the increasing use of such horns for calibration purposes.

B2. Basic Procedure. The horn gain is measured through a comparison of signal levels obtained in a direct connection vs a radiative connection, as shown in Fig. 16. The accuracy of the method is based on having a well calibrated r.f. attenuator and identical antennas.

The equations governing the comparison are:

$$P_r = \Gamma_l P_t \Gamma_g \quad \text{for direct connection and}$$

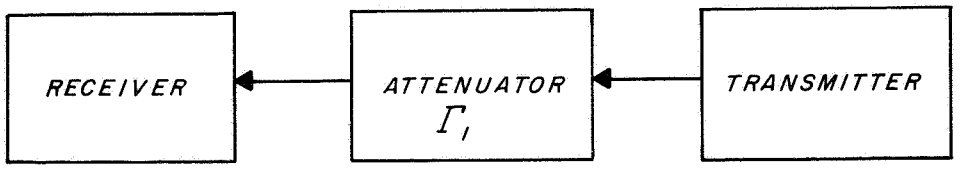

DIRECT CONNECTION

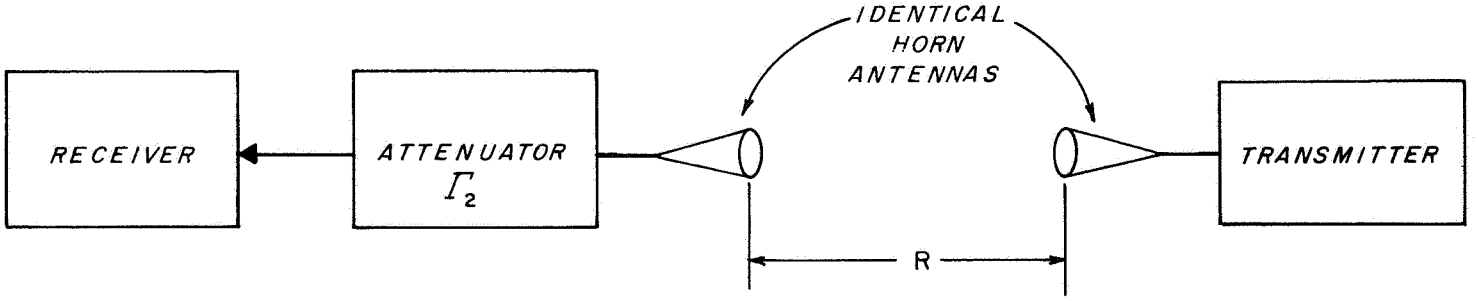

RADIATIVE CONNECTION

HORN GAIN MEASUREMENT

Fig. 16.

$$P_r = \frac{\Gamma_2 P_t \lambda^2 G^2}{(4\pi R)^2} \quad \text{for radiative connection}$$

where

P_r = r.f. power into receiver

P_t = transmitter power

λ = wavelength in meters

G = gain in dB/isotropic

R = distance between antennas

Γ_g = loss of waveguide in direct connection

Γ_1, Γ_2 = settings of r.f. attenuator for two cases.

The measurement procedure is as follows: With the direct connection a signal level of convenience is established as indicated by the video signal at the second detector of the receiver. Then a change is made to the radiative convection and the r.f. attenuator is adjusted to give the same power level. This should be done at a number of separation distances for self-consistency check on the data, but a measurement at any distance will suffice for a gain measurement. Equating the detector powers for the two types of connections, one finds the gain to be

$$G^2 = \frac{(4\pi R)^2}{\lambda^2} \quad \frac{\Gamma_g \Gamma_1}{\Gamma_2} .$$

Thus one can solve for the gain knowing the separation distance, the waveguide and attenuator losses, and the wavelength.

B3. Near Field Corrections. The nominal far field region, $2D^2/\lambda$, is 1.2 meters for the experiments. Since separations as close as .534 meters are used in the measurement, corrections for near field gain loss must be made. The near field correction enters into the gain expression through changing the total phase error, as discussed in the previous Appendix. These gain losses have been calculated and applied to the data. Fig. 17 shows the near field gain loss for the horn at λ = 4.3 mm.

B4. Phase Center Corrections. In the radiative convection, readings are taken at many separation distances. The equation governing this case shows that

$$\frac{R^2}{\Gamma_2} = \text{constant or } R \propto \sqrt{\Gamma_2}$$

Thus if we plot $\sqrt{\Gamma_2}$ vs R, we should get a straight line, except for experimental error. There are three reasons for doing so.

(1) By regressing the data, we can easily average all data points to improve the accuracy of the result.

(2) A self-consistency check on the data is obtained, including the near field corrections, which must be applied to the data before plotting.

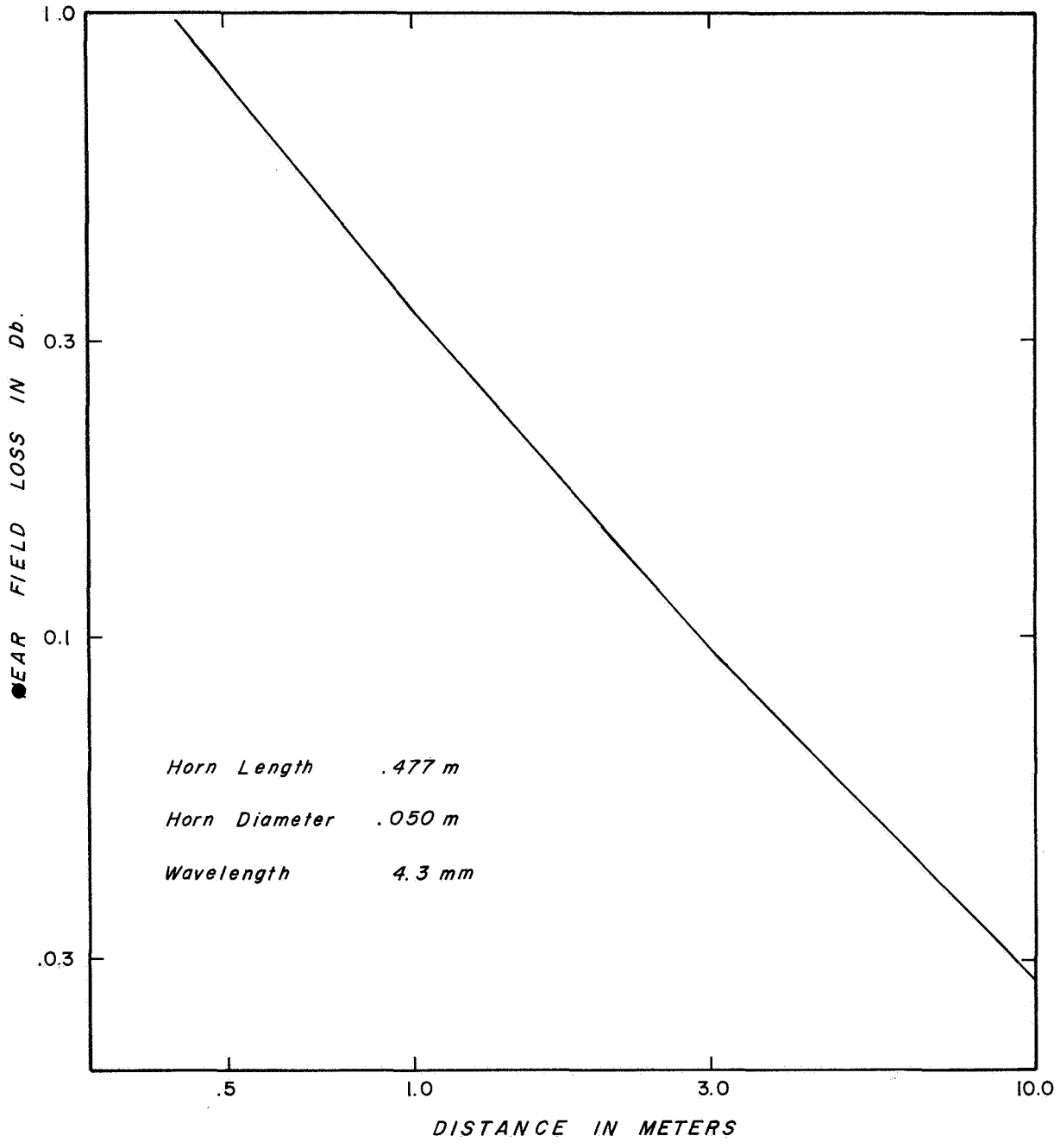

NEAR FIELD GAIN LOSS

Fig. 17.

(3) The exact phase centers of the antennas are difficult to estimate and thus the values of R used should be considered relative. The intercept with the R-axis should give a correction to the distance scale by indicating the exact phase center.

Fig. 18 shows some λ = 4.3 mm data plotted in the manner described. The phase center correction of approximately .09 meters is clearly indicated.

B5. Attenuator Calibration. The r.f. attenuators used in these tests were calibrated by the i.f. substitution method. The standard used was a 60 mHz cutoff attenuator manufactured by Airborne Instruments Laboratory. An accuracy of approximately .2 dB over the range used in this test is indicated by the specifications of the i.f. attenuator.

B6. Results. Only the 4.3 mm horn has been calibrated by the method described in this Appendix. The result of the calibration was 31.96 dB for the far-field gain. This is to be compared with the calculated value of 31.89 dB, differing by .07 dB or 1.4%. Whether this degree of accuracy is inherent in the methods used or is merely fortuitous remains to be determined as the other horns are measured.

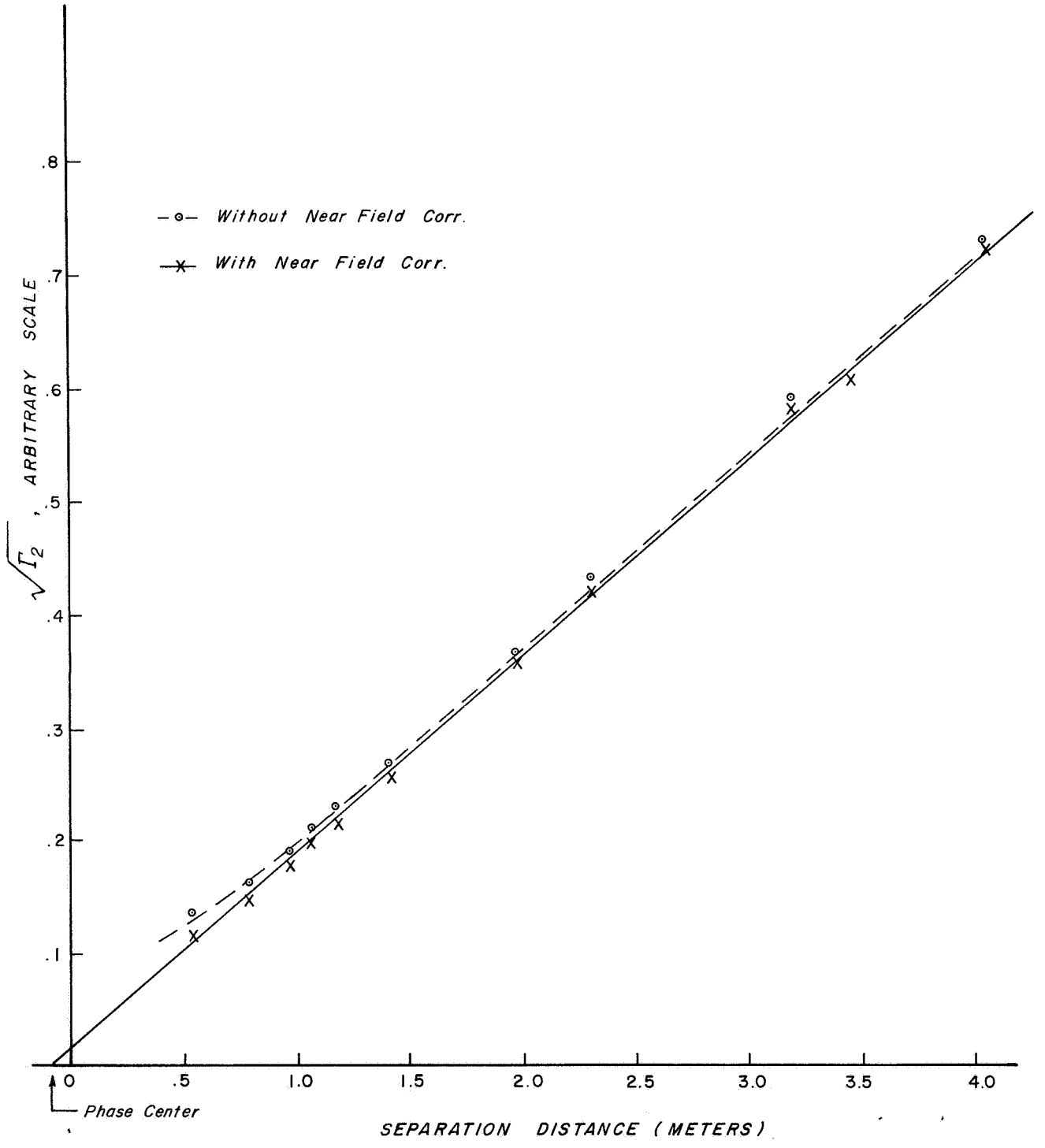

PHASE CENTER CORRECTION

Fig. 18.

REFERENCES

1. Tolbert, C. W., A. W. Straiton, and L. C. Krause, "A 16-Foot Diameter Millimeter Wavelength Antenna System, Its Characteristics and Applications," IEEE Transactions on Antennas and Propagation, Vol. AP-13, No. 2, pp. 225-229 (March 1965).

2. Tolbert, C. W., "Millimeter Wavelength Spectra of the Crab and Orion Nebulae," Nature, Vol. 206, No. 4991, pp. 1304-1307 (26 June 1965).

3. Tolbert, C. W., "Observed Millimeter Wavelength Brightness Temperatures of Mars, Jupiter, and Saturn," Astronomical Journal, Vol. 71, No. 1, pp. 30-32 (February 1966).

4. Takahashi, K., "An Investigation of the Solar Emission at Frequencies of 35 Gc, 70 Gc, and 94 Gc with a 4.88 Meter Diameter Telescope," The Astrophysical Journal, Vol. 148 (May 1967).

5. Clardy, D. E. and A. W. Straiton, "Radiometric Measurements of the Moon at 8.6 mm and 3.2 mm," Astrophysical Journal, Vol. 154, pp. 775-782 (November 1968).

6. Kuiper, G. P., "Planetary Atmospheres and Their Origin," The Atmospheres of the Earth and Planets, Chicago: University of Chicago Press, 1952 (Revised Edition), pp. 306-405.

7. Opik, E. J., "Jupiter: Chemical Composition, Structure, and Origin of a Giant Planet," Icarus, 1 (1962), pp. 200-257.

8. Thornton, D. D., and W. J. Welch, "8.35 mm Radio Emission from Jupiter," Icarus, 2 (1963), pp. 228-232.

9. Marcuvitz, Norman, Ed., Waveguide Handbook, McGraw-Hill Publishing Co., N. Y., 1951, pp. 196ff.

10. Silver, Samuel, Ed., Microwave Antenna Theory and Design, Boston Technical Publisher, Inc., 1964, pp. 158 ff.

11. Chu, L. J., "Calculation of the Radiation Properties of Hollow Pipes and Horns," Journal of Applied Physics, Vol. 11, pp. 603-610 (1940).

12. Silver, Samuel, op. cit., pp. 336-341.